C.P. No. 1241

PROCUREMENT EXECUTIVE, MINISTRY OF DEFENCE

AERONAUTICAL RESEARCH COUNCIL

CURRENT PAPERS

The Calculated Growth of Lift and Moment on a Swept Wing Entering a Discrete Vertical Gust at Subsonic Speeds

by

H. C. Garner

Aerodynamics Dept., R.A.E., Farnborough

LONDON: HER MAJESTY'S STATIONERY OFFICE

1973

PRICE 95 *p* NET

UDC 533.693.1 : 551.551 : 533.6.048.5 : 533.6.013.13 : 533.6.013.152

CP No.1241*
January 1972

THE CALCULATED GROWTH OF LIFT AND MOMENT ON A SWEPT WING ENTERING A DISCRETE VERTICAL GUST AT SUBSONIC SPEEDS

by

H. C. Garner

SUMMARY

Unsteady aerodynamic forces on a wing due to a uniform step gust are expressed as a sine transform of those due to sinusoidal gusts over the spectrum of wavelength. The sinusoidal gusts are treated by subsonic lifting-surface theory until the wavelength becomes so small as to demand excessive terms in the chordwise loading. Beyond this, the substitution of piston theory is discussed for a wing representative of design for subsonic cruise. Lift and pitching moment are calculated for normal entry into a step gust at Mach numbers 0.4 and 0.8, with reasonable success in the latter case. The results for small distances of penetration are examined critically. It is recommended that the proportional growth of aerodynamic force be taken between the results of piston theory and the present method for small distances before approaching the latter result, which leads to the correct asymptotic behaviour soon after the wing is completely immersed in the gust. The investigation ends with some calculations by the present method for normal entry into a ramp gust and by piston theory for oblique entry into a step gust.

---

* Replaces RAE Technical Report 72010 - ARC 33854

CONTENTS

1 INTRODUCTION

The study of aerodynamic forces on an aircraft in level flight in response to a sharp-edged up-gust is rightly associated with the name of Küssner[1] (1936), whose original solution to the problem of a uniform gust in twodimensional incompressible flow opened up an extensive field of research. The Küssner function for the growth of lift in terms of the distance travelled into the gust has been determined under more general conditions, and an account of the developments up to about 1955 is given by Lomax[2]. He refers to theoretical studies in twodimensional compressible flow and in threedimensional supersonic flow and to the lack of solutions for threedimensional subsonic flow. Considerable difficulties have subsequently been encountered in seeking numerical solutions for wings in subsonic flight. On the assumption that linear principles can be applied, there are several distinct approaches to this aerodynamic problem, most of which involve integrals of superposition over the frequency spectrum (section 2). A promising method from the numerical standpoint is to combine results for sinusoidal gusts of wavelengths from zero to infinity.

In practical applications to transient aircraft response, Mitchell[3,4] has introduced a Fourier transform method to avoid the direct evaluation of the Küssner functions. Whilst such an approach is highly desirable, it may tend to gloss over any inaccuracies implicit in the treatment of the aerodynamics. It therefore remains necessary to be able to examine the forcing terms due to the gust, as derived from the available oscillatory aerodynamic data. This Report, being a detailed study of the accuracy in calculating these terms, makes no further reference to aircraft response and excludes all structural considerations; it concerns the dynamics of the air and not of the aircraft.

The linearized lifting-surface method of Ref.5 is used because of its capability up to frequencies outside the flutter range. However, limitations do arise at very high frequency (section 3.1) and the hope is that in this extreme range it might prove satisfactory to substitute piston theory (section 3.2). Imperfections in this procedure are readily detected and receive critical discussion (section 3.3) with serious implications at small Mach number. Application is made to the planform in Fig.1a of aspect ratio 6, taper ratio 1/3 and mid-chord sweepback 30° at Mach numbers of 0.4 and 0.8 Very few previous attempts, if any, have been made to evaluate the gust-induced loading on such a planform, chosen to be typical of design for high subsonic cruise.

The basic calculations for sinusoidal gusts are built into results for a normal step gust, that is, a stationary uniform up-gust with its front in a plane normal to the flight path (section 4.1); the most precarious part of the calculation concerns small distances of penetration. It is a simple matter of superposition to form a normal ramp gust (Fig.1b); in the results, so deduced, the imperfections become much less noticeable (section 4.2). The case of an oblique step gust with arbitrary inclination of the vertical gust front to the flight path (Fig.1c) is only considered qualitatively by piston theory (section 4.3). The normalized Kussner functions then show no effect of Mach number but are expected to become increasingly unreliable at the lower speeds of flight.

2 CHOICE OF METHOD

Consider a wing in level flight at velocity U inclined at an angle ψ to the normal to the vertical front of an up-gust of uniform velocity w_g. In the notation of Fig.1c, let

$$x - y \tan \psi = \sigma \bar{c} \tag{1}$$

define the gust front relative to the wing of geometric mean chord $\bar{c}$ after its leading apex (or origin of planform) has travelled a distance

$$\sigma \bar{c} = Ut \tag{2}$$

since entering the gust at time $t = 0$. Then the boundary condition on the wing is simply

$$\left.\begin{aligned} w &= w_g \qquad (x - y \tan \psi < \sigma \bar{c}) \\ w &= 0 \qquad (x - y \tan \psi > \sigma \bar{c}) \end{aligned}\right\} . \tag{3}$$

In the following treatment of this boundary condition it is convenient to choose the origin so that no part of the planform has entered the gust when $\sigma = 0$. By virtue of the well-known identity

$$\int_0^\infty \frac{\sin bx}{x}\, dx = \pm \tfrac{1}{2}\pi \quad \text{according as} \quad b > \text{ or } < 0 \ , \tag{4}$$

with $b\bar{c} = x - y \tan \psi \pm \sigma \bar{c}$, equation (3) can be replaced by

$$\frac{w}{w_g} = \frac{1}{2\pi}\int_{-\infty}^{\infty} \exp\left\{\frac{i\bar{\nu}}{\bar{c}}(x - y\tan\psi)\right\}\frac{\sin\bar{\nu}\sigma}{\bar{\nu}}\,d\bar{\nu}$$

$$+\left[\frac{1}{2} + \frac{i}{2\pi}\int_{-\infty}^{\infty} \exp\left\{\frac{i\bar{\nu}}{\bar{c}}(x - y\tan\psi)\right\}\frac{\cos\bar{\nu}\sigma}{\bar{\nu}}\,d\bar{\nu}\right] . \qquad (5)$$

The two parts of equation (5) contribute equally to w in the region $x - y\tan\psi > -\sigma\bar{c}$, while only the square bracket contributes to $w = w_g$ where $x - y\tan\psi < -\sigma\bar{c}$. In this latter range upstream of the wing the behaviour of w is immaterial; therefore for $\sigma \geqslant 0$

$$\frac{w}{w_g} = \frac{1}{\pi}\int_{-\infty}^{\infty} \exp\left\{\frac{i\bar{\nu}}{\bar{c}}(x - y\tan\psi)\right\}\frac{\sin\bar{\nu}\sigma}{\bar{\nu}}\,d\bar{\nu} \qquad (6)$$

and

$$\frac{w}{w_g} = 1 + \frac{i}{\pi}\int_{-\infty}^{\infty} \exp\left\{\frac{i\bar{\nu}}{\bar{c}}(x - y\tan\psi)\right\}\frac{\cos\bar{\nu}\sigma}{\bar{\nu}}\,d\bar{\nu} \qquad (7)$$

may be regarded as alternative expressions equivalent to equation (3) or (5).

The most straightforward approach to the evaluation of the unsteady wing loading associated with equation (3) is first to solve the oscillatory problem with circular frequency $\omega = U\bar{\nu}/\bar{c}$ for a sinusoidal gust with boundary condition

$$\frac{W}{U} = \exp\left\{\frac{i\bar{\nu}}{\bar{c}}(x - y\tan\psi)\right\} . \qquad (8)$$

Let $Q_i(\bar{\nu})$ be the corresponding coefficient of generalized force in some mode of vertical displacement $z_i(x,y)$. Then the unsteady generalized force due to the step gust

$$Q_{ig}(\sigma) = \frac{w_g}{U}\left[\frac{1}{2\pi}\int_{-\infty}^{\infty}\frac{Q_i(\bar{\nu})\sin\bar{\nu}\sigma}{\bar{\nu}}\,d\bar{\nu} + \tfrac{1}{2}Q_i(0) + \frac{i}{2\pi}\int_{-\infty}^{\infty}\frac{Q_1(\bar{\nu})\cos\bar{\nu}\sigma}{\bar{\nu}}\,d\bar{\nu}\right]$$

$$= \frac{w_g}{U}\left[\tfrac{1}{2}Q_1(0) + \frac{i}{2\pi}\int_{-\infty}^{\infty}\frac{Q_i(\bar{\nu})}{\bar{\nu}}e^{-i\bar{\nu}\sigma}d\bar{\nu}\right]$$

$$= \frac{w_g}{U}\left[Q_i(0) + \frac{i}{2\pi}\int_{-\infty}^{\infty}\frac{Q_i(\bar{\nu}) - Q_1(0)}{\bar{\nu}}e^{-i\bar{\nu}\sigma}d\bar{\nu}\right] \qquad (9)$$

is derived for $\sigma > 0$ by superposition from equation (5). This is essentially the form of Kussner function given by Drischler in equation (8) of Ref.6 and used in his calculations. The results for normal gusts in subsonic flow in Appendix A of Ref.6 are restricted to unswept wings with approximate expressions

$$Q_i(\bar{\nu}) - Q_i(0) = i\bar{\nu} \sum_n \frac{a_n}{b_n + i\bar{\nu}} \tag{10}$$

to represent the generalized force over the frequency spectrum. However, there does not appear to be any justification for this form of series in compressible flow when the frequency parameter is large.

An alternative approach, used by Drischler and Diederich in the appendix to Ref.7, is to represent the boundary conditions of the step gust in terms of those for leading-edge flaps with hinge lines parallel to the gust front. From a knowledge of the generalized force for flaps of various sizes in plunging motion at sufficient values of the frequency parameter, it is possible to evaluate a double integral for $Q_{ig}(\sigma)$. This 'plunging-flap' method has been applied successfully to twodimensional problems, but it is less suitable for wings of finite aspect ratio. Although the downwash mode becomes independent of frequency parameter, the discontinuity in boundary condition at the flap hinge is a severe complication and a likely source of inaccuracy. Another scheme of calculation involves the reverse-flow theorem, by which the sinusoidal-gust and the plunging-flap methods can be shown to be equivalent. However, in the context of equation (9), the reverse flow merely offers an alternative calculation of $Q_i(\bar{\nu})$ with no obvious improvement. Nevertheless, for any particular mode $z_i(x,y)$, there might be some economy in that the same set of solutions with different $\bar{\nu}$ for the reversed planform could be utilized, whatever the gust inclination ψ.

Unlike the methods mentioned above for subsonic compressible flow, there is one that involves a general relation between the downwash and the load distribution with arbitrary time dependence. In equation (15) of Ref.8, Drischler presents a triple integral in one time and two spatial variables for $w(x,y,t)$ in terms of the unknown load distribution and its history. Although it is claimed that the integral should lend itself readily to modern high-speed computing machines, the present author is not aware of any such application to finite wings in compressible flow. Apart from linearization, the equation is all-embracing and remarkably compact. It is particularly instructive how the

circular spatial region of integration relates to the travel of acoustic waves from the pressure disturbances, as this physical feature of the aerodynamics is quite unrecognizable in equation (9).

Because the recent development of a lifting-surface method for general frequency in Ref.5 gave the opportunity to calculate $Q_i(\bar{\nu})$ with more reliability than was possible formerly, the sinusoidal-gust approach has been chosen for the present investigation. In place of equation (9), equivalent expressions for $Q_{ig}(\sigma)$ are obtained by combining equation (8) with the alternative expressions (6) and (7) for w/w_g to give respectively

$$Q_{ig} = \frac{w_g}{\pi U} \int_{-\infty}^{\infty} \frac{Q_i(\bar{\nu}) \sin \bar{\nu}\sigma}{\bar{\nu}} d\bar{\nu} \tag{11}$$

and

$$Q_{ig} = \frac{w_g}{U} \left[Q_i(0) + \frac{1}{\pi} \int_{-\infty}^{\infty} \frac{Q_i(\bar{\nu}) \cos \bar{\nu}\sigma}{\bar{\nu}} d\bar{\nu} \right] . \tag{12}$$

With a change of notation from that of Ref.5, it is convenient to separate $Q_i(\bar{\nu})$ into its real and imaginary parts by writing

$$Q_i(\bar{\nu}) = Q_i'(\bar{\nu}) + iQ_i''(\bar{\nu}) , \tag{13}$$

where $Q_i'(\bar{\nu})$ is an even function of $\bar{\nu}$ and $Q_i''(\bar{\nu})$ is an odd function. The normalized Küssner function is used when the steady-state value

$$Q_{ig}(\infty) = \frac{w_g}{U} Q_i'(0) \tag{14}$$

is non-zero; from equations (11) to (14) we write

$$k_i(\sigma) = \frac{Q_{ig}(\sigma)}{Q_{ig}(\infty)} = \frac{2}{\pi} \int_0^{\infty} \frac{Q_i'(\bar{\nu})}{Q_i'(0)} \frac{\sin \bar{\nu}\sigma}{\bar{\nu}} d\bar{\nu} \tag{15}$$

and alternatively

$$k_i(\sigma) = 1 - \frac{2}{\pi} \int_0^{\infty} \frac{Q_i''(\bar{\nu})}{Q_i'(0)} \frac{\cos \bar{\nu}\sigma}{\bar{\nu}} d\bar{\nu} . \tag{16}$$

Mitchell[9] has derived and calculated the transient forces from similar equations. Equation (16) corresponds to equation (8a) of Ref.9, while equation (15) is equivalent to Mitchell's equation (8b) when the sign of the integral is corrected. His technique is to truncate the upper range of integration in equations (15) and (16) in a careful manner, but this involves some extrapolation beyond the values of $\bar{\nu}$ for which the theoretical data for $Q_i(\bar{\nu})$ are reliable. It is important to note that, for small values of σ at least, equation (16) gives $k_i(\sigma)$ as the difference between two nearly equal quantities and only small percentage errors in the integral can be tolerated. The integral in equation (15) is less critical in this respect; it automatically vanishes when $\sigma = 0$ and is therefore preferred to equation (16).

3 NUMERICAL PROCEDURE

The evaluation of equation (15) falls naturally into three parts. The first stage is the calculation of $Q_i'(\bar{\nu})$, the real part of the generalized force in some mode $z_i(x,y)$ corresponding to the sinusoidal gust defined in equation (8). While it is clear from section 2 that the formulation is basically unaltered by the inclination of the gust front, the calculations by lifting-surface theory[5] in section 3.1 are limited to the symmetrical case $\psi = 0$. Being a collocation method, Ref.5 will inevitably fail if $\bar{\nu}$ is too large. Rather than truncate the integral in equation (8), as Mitchell[9] did, we approximate to the integrand by means of piston theory and seek to justify this in section 3.2. Finally, in section 3.3, the accuracy of integration is discussed and difficulties in reconciling equations (15) and (16) are brought to light.

3.1 Sinusoidal gust

Consider the case of a normal gust when equation (8) reduces to

$$\frac{W}{U} = e^{i\bar{\nu}x/\bar{c}} \quad . \tag{17}$$

In applying section 4.2 of Ref.5 to the wing in Fig.1a, the planform area $S = 2s\bar{c}$ is taken as reference area and geometric mean chord $\bar{c}$ as reference length. Thus

$$Q_i = -\frac{1}{2S\bar{c}} \iint_S z_i(x,y)\ell(x,y)\,dxdy \tag{18}$$

where the lift per unit area as a fraction of the dynamic pressure $\frac{1}{2}\rho U^2$ is written as

$$\ell(x,y) = \frac{8s}{\pi c(y)} \sum_{q=1}^{N} \Gamma_q(y) \frac{\cos (q-1)\phi + \cos q\phi}{\sin \phi} \tag{19}$$

with

$$x = x_\ell(y) + \tfrac{1}{2}c(y)(1 - \cos \phi) \quad . \tag{20}$$

The planform has central rounding, as specified in section 5.4 of Ref.5, to ensure that the leading edge $x_\ell(y)$ and chord $c(y)$ have continuous second derivatives. The N spanwise loading functions in equation (19) are expressed as

$$\Gamma_q(y) = \frac{2}{m+1} \sum_{r=1}^{m} \left[\Gamma_{qr} \sum_{\mu=1}^{m} \sin \mu\theta \sin \mu\theta_r \right] \tag{21}$$

in terms of their values Γ_{qr} at the m collocation sections

$$y = y_r = -s \cos\left(\frac{r\pi}{m+1}\right) = -s \cos \theta_r \tag{22}$$

and as functions of

$$\theta = \cos^{-1}\left(-\frac{y}{s}\right) . \tag{23}$$

We consider two force modes $z_i(x,y)$, namely

$$\left.\begin{aligned} z_1 &= -\bar{c} \quad \text{(lift)} \\ z_2 &= -(x - x_0) \quad \text{(negative pitching moment)} \end{aligned}\right\} , \tag{24}$$

where the pitching axis $x = x_0$ will be either at the root leading edge ($x_0 = 0$) or at the aerodynamic centre.

No attempt will be made here to describe the method of Ref.5 in any detail. Suffice it to say that the modified downwash

$$\frac{\bar{w}}{U} = \frac{w}{U} e^{i\bar{\nu}x/\bar{c}} \tag{25}$$

corresponding to the loading in equation (19) is evaluated as a double integral with

$$\Lambda = a(m + 1) - 1 \tag{26}$$

spanwise integration points and is then equated to the value from equation (17)

$$\frac{\bar{w}}{U} = \frac{W}{U} e^{i\bar{\nu}x/\bar{c}} = e^{2i\bar{\nu}x/\bar{c}} \tag{27}$$

at each of the mN collocation points given by

$$\left.\begin{aligned} x &= x_{p\nu} = x_{\ell}(y_{\nu}) + \tfrac{1}{2}c(y_{\nu})(1 - \cos\phi_p) \\ y &= y_{\nu} = -s\cos\left(\frac{\nu\pi}{m+1}\right), \qquad \nu = 1(1)m \\ \phi_p &= \frac{2\pi p}{2N+1}, \qquad p = 1(1)N \end{aligned}\right\} . \tag{28}$$

The resulting complex linear simultaneous equations are solved for the unknown coefficients Γ_{qr}, so that the nondimensional generalized forces Q_i can be evaluated from equations (18) to (24). The procedure involves the three arbitrary positive integers from equations (26) and (28), (N,m,a), each of which must be large enough to achieve the desired numerical convergence. As a computational aid to the evaluation of the required input data W/U from equation (17), it proved convenient to use the output data $\bar{w}/U$ of equation (25) resulting from the simpler input $w/U = 1$.

Guide lines for the selection of a suitable combination of integers (N,m,a) are summarized by the following inequalities from section 4.3 of Ref.5:

$$\left.\begin{aligned} N &> 2 + \sigma + \frac{2\bar{\nu}}{\pi} \\ m &\geqslant 10 \\ m &> \tau + \frac{4sc_R}{\bar{c}^2}\sec\Lambda_t \\ a(m+1) &> (2N-4)(1+2A) \end{aligned}\right\} , \tag{29}$$

where the polynomial $(x/\bar{c})^{\sigma}(y/s)^{\tau}$ indicates the nature of the mode of oscillation and respectively s, c_R, Λ_t and A denote semi-span, root chord, trailing edge sweepback and aspect ratio of the planform. If these inequalities

are satisfied, roughly three-figure accuracy should be obtainable. In the present circumstances $\tau = 0$ and $m = 20$ should suffice for the planform data of Fig.1a. The condition on N is less clear-cut, but if we assign the value $\sigma = 2\bar{\nu}/\pi$ as being representative of equation (17), $N = 6$ together with $a = 5$ would satisfy the conditions for frequency parameters up to $\bar{\nu} = \pi$. Above $\bar{\nu} = \frac{3}{2}\pi$, however, $N \geqslant 9$ with $a \geqslant 9$ would be required, and the combination $(N,m,a) = (9,20,9)$ exceeds the storage limit of the KDF9 computer in the time-sharing mode and would otherwise involve an excessive running time of about 3 hours. Although the problem of accuracy in the evaluation of $Q_1(\bar{\nu})$ is greatly aggravated by the large aspect ratio $A = 6$, this has merely lowered the value of $\bar{\nu}$ above which the program of Ref.5 ceases to be reliable. Whatever the aspect ratio, some compromise in accuracy would be necessary.

Like the majority of the pitching derivatives for the same planform in section 5.4 of Ref.5, the present calculations for $M = 0.4$ and 0.8 have been made for a combination of integers $(N,m,a) = (6,15,4)$ that falls somewhat short of the conditions (29). The frequency parameters are taken from the formula

$$\bar{\nu} = \bar{\nu}_f = \tfrac{1}{2}\cot\left(\frac{\pi}{20}\right)\tan\left(\frac{\pi f}{20}\right), \qquad (30)$$

such that the finite range $0 \leqslant f \leqslant 10$ covers the whole frequency spectrum and the results for Q_1 and $-Q_2'$ in Tables 1 and 2 correspond to $f = 0, \frac{1}{2}, 1, 2, 3, 4, 5, 6, 6\frac{1}{2}$ and 7. From the study of convergence in Ref.5, it appears that the pitching derivatives begin to show significant inaccuracies at $\bar{\nu} = 4.345 (f = 6)$. The evidence in Table 6 of Ref.5 is that the effect of increasing N above 6 is more important than that of increasing a above 4 and may expose errors of the order 2%. Moreover, Table 5 of Ref.5 indicates the possibility of similar changes in pitching derivatives when m is increased above 15. It is envisaged that the value of N would need to be greater to cope with the wavy mode of a sinusoidal gust than with the linear mode of pitching. However, the following calculations for $M = 0.4$ and $\bar{\nu} = 3.157 (f = 5)$

(N,m,a)	Q_1	$Q_2(x_0 = 0)$
(6,15,4)	0.3906 - i 1.0844	1.3626 - i 0.7008
(7,15,4)	0.3920 - i 1.0814	1.3633 - i 0.6986

suggest that $N = 6$ is adequate up to that frequency parameter. Accordingly, we use the data in Tables 1 and 2 with the proviso that they become less and less reliable as $\bar{\nu}$ increases beyond the flutter range; thus the results for the three highest frequencies are treated with reserve.

The real component of Q_1 is plotted against $\bar{\nu}$ for $M = 0.4$ and $M = 0.8$ to produce the undulating full curves in Fig.2. There is a tendency for the reversals of sign to occur at lower frequencies for the lower Mach number. Comparable curves by Murrow *et al.*[10] are available for a very limited range of frequency parameter $k = \frac{1}{2}\omega c_R/U$. From the upper curves of Figs.2e and 2f of Ref.10, it is interesting to note that the real part of the lift for $M = 0.4$ reverses sign at

$$\bar{\nu} = \frac{2\bar{c}k}{c_R} = 1.42k = 1.1 \qquad \text{when} \quad A = 4$$

and at about $\bar{\nu} = 0.6$ when $A = 9.43$. For the same order of sweepback and taper, the intermediate reversal point $\bar{\nu} = 0.85$ from the present calculations of Q_1' for $A = 6$ confirms the trend that frequency effects are more pronounced at the higher aspect ratios. On the other hand, the quarter-chord sweepback of 33.5° is a contributory factor, as other results in Fig.2 of Ref.10 show. Indeed the larger streamwise extent of the wing as a fraction of the wavelength $2\pi\bar{c}/\bar{\nu}$ of the sinusoidal gust would be expected to encourage the undulations in the present Fig.2. The more important part of the frequency range is adequately covered, and the remainder $\bar{\nu} \geqslant 4.345$ is hardly expected to influence the aerodynamic loading due to a step gust once the wing is immersed.

3.2 Piston theory

The introduction of piston theory[11,12] into the present discussion has a threefold purpose. It is used in an attempt to offset the deficiencies of the subsonic lifting-surface method in the upper range of frequency: it is a common tool in calculations of gust loading in the absence of other theoretical data, and here is the opportunity to judge its effectiveness: it serves to provide rough estimates of the aerodynamic forces induced by an oblique gust, which is not covered by the present lifting-surface calculations.

The relevant equations from piston theory are derived in the appendix. Although its applicability to oscillatory flow is subject to the severe restrictions

$$\left.\begin{aligned} \bar{\nu}M &\gg 1 \\ A\bar{\nu}M &\gg 1 \end{aligned}\right\} , \tag{31}$$

there must exist an upper range of frequency parameters in which the theory is valid when $M > 0$. The nondimensional complex lift $Q_1(\bar{\nu})$ and the real part of $Q_2(\bar{\nu})$ from equations (A-7) to (A-9) of the appendix are inversely proportional to M and are evaluated for $M = 0.8$ in Tables 1 and 2. Although it is fortuitous that $Q_1'(0)$ is so close to the present lifting-surface value for $M = 0.8$, the remarkable agreement between the two curves of $Q_1'(\bar{\nu})$ in Fig.2 at the high-frequency end encourages us to use piston theory for the whole upper range $\bar{\nu} \geqslant 4.345 (f \geqslant 6)$. The justification for this procedure at the lower Mach number $M = 0.4$ is less convincing, because the conditions (31) for the validity of piston theory are more stringent and discrepancies are apparent in the upper diagram of Fig.2. Nevertheless, the appeal to piston theory is further supported by the fact that the frequent changes in the sign of the real parts of equations (A-7) to (A-9) ensure that their contributions to equation (15) in the upper range of integration are minor ones.

With regard to the use of piston theory in its own right, expressions for the normalized Küssner functions $k_1(\sigma)$ and $k_2(\sigma)$ in the special case $\psi = 0$ are derived as exact polynomials in σ in equations (A-12) and (A-13) respectively. The formulae change whenever a corner of the planform enters the gust. The corresponding functions for an oblique gust are less convenient to formulate, but a procedure for their calculation is described in the appendix in four stages through equations (A-14) to (A-23). The lift is still quadratic in σ, while the moments remain cubic functions. Without prejudice to the argument in section 2, the origin is taken at the root leading edge. Thus, when $\psi > \Lambda_\ell$, the wing tip enters the gust while $\sigma < 0$ (Fig.1c). The final equations (A-22) and (A-23) give expressions for

$$\frac{C_m}{C_{L\infty}} \quad \text{and} \quad \frac{C_\ell}{C_{L\infty}} ,$$

where

$$\left.\begin{aligned} C_m &= \frac{\text{nose-up pitching moment about } x = x_0}{\tfrac{1}{2}\rho U^2 S\bar{c}} \\ C_\ell &= \frac{\text{port-wing-up rolling moment}}{\rho U^2 Ss} \\ C_{L\infty} &= 2Q_1(0) \text{ is the final lift coefficient} \end{aligned}\right\} . \qquad (32)$$

It is convenient to take the pitching axis through the aerodynamic centre $x_0 = x_{ac}$ such that $Q_2(0) = 0$. Then both pitching and rolling moments can be treated as transient functions that disappear as soon as the wing is fully immersed in the gust.

3.3 Evaluation of integral

Irrespective of the undulations in $Q_1'(\bar{\nu})$ for large $\bar{\nu}$, the factor $\sin \bar{\nu}\sigma$ in the integrand of equation (15) becomes highly oscillatory in this region and complicates numerical integration, especially when σ is large. A possible way round the difficulty is to express $Q_i(\bar{\nu})$ in the form of equation (10) and thereafter use exact integration. This approach was rejected, as it had been found unsuitable in a previous investigation and as it did not appear to be compatible with equations (A-7) to (A-9). Instead, numerical integrations of two types were considered. Firstly, for small σ, the whole integrand was treated by Simpson's rule after transformation to the independent variable f. Thus by equations (15) and (30)

$$k_1(\sigma) = \frac{2}{\pi} \int_0^{10} \frac{Q_i'(\bar{\nu})}{Q_1'(0)} \frac{\sin \bar{\nu}\sigma}{\bar{\nu}} \frac{d\bar{\nu}}{df}\, df \quad , \qquad (33)$$

where

$$\frac{d\bar{\nu}}{df} = \frac{\pi}{40} \cot\left(\frac{\pi}{20}\right) \sec^2\left(\frac{\pi f}{20}\right) = \frac{\pi}{40}\left[\cot\left(\frac{\pi}{20}\right) + 4\bar{\nu}^2 \tan\left(\frac{\pi}{20}\right)\right] . \qquad (34)$$

The range $0 < f < 6$ was handled by careful interpolation in Tables 1 and 2 to give values in steps of $\frac{1}{4}$. Secondly, for large σ and $\bar{\nu}$, consistent polynomials for $Q_i'(\bar{\nu})/\bar{\nu}$ were taken over the same intervals and exact integrations with respect to $\bar{\nu}$ were formulated and evaluated. The discrepancies between the two methods were never very large, and the latter one was only found to be necessary in a few instances.

As explained in section 3.2, the range $5 < f < 6$ is used to fair $Q_i'(\bar{\nu})$ into its value from piston theory. Equation (33) is then re-written as

$$k_i(\sigma) = \frac{2}{\pi}\int_0^{\infty} \frac{\bar{Q}_i'(\bar{\nu})}{Q_i'(0)} \frac{\sin \bar{\nu}\sigma}{\bar{\nu}}\, d\bar{\nu} + \frac{2}{\pi}\int_0^{10} \frac{Q_i'(\bar{\nu}) - \bar{Q}_i'(\bar{\nu})}{Q_i'(0)} \frac{\sin \bar{\nu}\sigma}{\bar{\nu}} \frac{d\bar{\nu}}{df}\, df$$

$$= \frac{\bar{Q}_i'(0)}{Q_i'(0)} \bar{k}_i(\sigma) + \frac{2}{\pi}\int_0^{6} \frac{Q_1'(\bar{\nu}) - \bar{Q}_i'(\bar{\nu})}{Q_1'(0)} \frac{\sin \bar{\nu}\sigma}{\bar{\nu}} \frac{d\bar{\nu}}{df}\, df \quad , \qquad (35)$$

where $\bar{Q}_i'(\bar{\nu})$ and $\bar{k}_i(\sigma)$ here denote the quantities from piston theory in equations (A-7) to (A-9), (A-12) and (A-13) to distinguish them from those calculated by the present method. While most of the calculations have been based on equation (35), the upper limit of integration is arbitrary. It must be neither so low that the approximation $Q_1'(\bar{\nu}) = \bar{Q}_i'(\bar{\nu})$ is unacceptable at that limit, nor so high that the calculated values $Q_1'(\bar{\nu})$ become unacceptable below that limit. It is already apparent from Fig.2 that this dilemma may be troublesome at $M = 0.4$, if not at $M = 0.8$.

As explained at the end of section 2, the alternative equation (16) for $k_i(\sigma)$ is regarded as having less numerical potential than equation (15). The corresponding alternative to equation (35) is

$$k_i(\sigma) = 1 + \frac{\bar{Q}_i'(0)}{Q_i'(0)} [\bar{k}_i(\sigma) - 1] - \frac{2}{\pi}\int_0^{6} \frac{Q_i''(\bar{\nu}) - \bar{Q}_i''(\bar{\nu})}{Q_i'(0)} \frac{\cos \bar{\nu}\sigma}{\bar{\nu}} \frac{d\bar{\nu}}{df}\, df \quad , \qquad (36)$$

and the consequences of its direct calculation will be examined briefly in section 4.1.

Particular attention is now given to the identity that follows from the limits of equations (15) and (16) as σ tends to zero. Equation (15) gives $k_i(0) = 0$, and the resulting integral from equation (16) must satisfy the condition

$$\frac{2}{\pi Q_i'(0)}\int_0^{\infty} \frac{Q_i''(\bar{\nu})}{\bar{\nu}}\, d\bar{\nu} = 1 \quad . \qquad (37)$$

It can be verified that equation (A-7) from piston theory satisfies equation (37) and indeed that the integral lies within 1% of its correct value if the infinite upper limit is replaced by any value of $\bar{\nu} > 3$. Each set of data in Table 1 is used to evaluate the lift integral ($i = 1$) with variable upper limit, as tabulated below.

Method	$\bar{\nu}$ / M	Value of integral (37) for upper limit $\bar{\nu}$				
		1.026	1.609	2.294	3.157	4.345
Piston theory	Any	0.805	1.001	1.033	0.998	0.999
Present theory	0.8	0.639	0.815	0.841	0.804	0.802
Present theory	0.4	0.795	0.946	0.878	0.740	0.700

The situation for $M = 0.8$ is easy to visualize in relation to piston theory. The steady-state quantity $Q_1'(0)$ is much the same in the two cases and, throughout the range $0 < \bar{\nu} < 4.345$, $Q_1''(\bar{\nu}) < \bar{Q}_1''(\bar{\nu})$ from piston theory. Accordingly the integral from the present theory is on the small side. To recoup the additional amount 0.197 from the range $\bar{\nu} > 4.345$, it would seem necessary not only that $[Q_1''(\bar{\nu}) - \bar{Q}_1''(\bar{\nu})]$ should change sign, as it does in Table 1, but also that this positive difference should continue to grow before tending slowly, perhaps logarithmically, to zero. This would seem to contradict the validity of piston theory until the frequency parameter is several orders of magnitude higher than the value 4.345. The situation for $M = 0.4$ in the table is even less satisfactory. Because we place less reliance in piston theory at this lower Mach number, it is perhaps easier to accept the deficit of 0.300 that is required to satisfy equation (37). This deficit, however, is the value $k_1(0)$ as calculated from equation (36), which must clearly be rejected unless σ is large enough to prohibit significant contributions from the upper range of frequency $6 < f < 10$. It is recognized that inaccuracies in $Q_1''(\bar{\nu})$ at high $\bar{\nu}$ probably imply inaccuracies also in $Q_1'(\bar{\nu})$, so that considerable care must be taken in interpreting the calculated Küssner functions for small σ from equation (35).

Rigorous justification of the present method for small as well as large σ would demand overlapping lower and upper ranges of $\bar{\nu}$ where respectively the lifting-surface method and piston theory apply. The failure to satisfy equation (37) implies a gap between these ranges, which can only be bridged by more elaborate collocation solutions over a substantial range of high frequency

parameter. The identity (37) seems to pose the ultimate challenge to any who seek to improve the numerical techniques of solving the linear problems of a rapidly-oscillating lifting surface in subsonic flow.

4 DISCUSSION OF RESULTS

The method of calculation, expressed in equation (35), has been applied to the tapered swept wing of Fig.1a entering a normal step gust. The results for lift and pitching moment are presented and appraised in section 4.1; consideration is given to the rate of propagation of disturbances on the wing and to anomalies in the calculations for small time. The corresponding functions for a normal ramp gust are derived in section 4.2, and in section 4.3 the case of an oblique step gust is considered approximately on the principle of piston theory.

4.1 Normal step gust

The Küssner functions, $k_1(\sigma)$ for lift and $k_2(\sigma)$ for pitching moment about the axis through the root leading edge, have been calculated from equation (35) for the two Mach numbers 0.4 and 0.8, and also from equations (A-12) and (A-13) of piston theory which are more suitable for higher Mach numbers. The results in the range $\sigma \leqslant 8$ are listed in Table 3 and presented graphically in Figs.3 and 4. The three regions of particular interest are

σ small, when most of the wing has still to enter the gust,

$\sigma \approx 2.73$, at which the wing becomes fully immersed,

σ large, when the steady state is approached asymptotically.

We consider these in the reverse order, starting with demonstrable precision and ending with inconsistencies that are difficult to interpret.

The only complication where σ is large is that the integrand of equation (35) becomes highly oscillatory. Special care in numerical integration is needed with resort to the second procedure mentioned below equation (34). However, the factor $\sin(\bar{\nu}\sigma)/\bar{\nu}$ ensures that the result is insensitive to the problematical values of $Q_i'(\bar{\nu})$ when $\bar{\nu}$ is large. The asymptotic form of $k_i(\sigma)$ for subsonic flow is known exactly from the analysis of Garner and Milne[13]. Equation (26) of Ref.13 (with subscript J omitted for a uniform gust) gives

$$k_1(\sigma) \sim 1 - \frac{AQ_1'(0)}{8\pi\sigma^2} + O(\sigma^{-3}) \quad . \tag{38}$$

Thus to order σ^{-2} the asymptotic curve of $k_i(\sigma)$ is independent of i, and we obtain

$$\left.\begin{aligned} &\text{for } M = 0.4 \ , \ k_i(\sigma) \sim 1 - 0.5008\sigma^{-2} \\ &\text{for } M = 0.8 \ , \ k_i(\sigma) \sim 1 - 0.6089\sigma^{-2} \end{aligned}\right\} \quad . \tag{39}$$

When results from Table 3 and equations (39) are compared in the following table, the agreement is fairly convincing.

M	σ	Table 3		Eqn. (39) $k_i(\sigma)$
		$k_1(\sigma)$	$k_2(\sigma)$	
0.4	6	0.987	0.985	0.986
0.4	8	0.994	0.994	0.992
0.8	6	0.980	0.980	0.983
0.8	8	0.990	0.990	0.990

A corollary to equation (38) is that the transient pitching moment about the aerodynamic centre is only of order σ^{-3} as the steady state is approached.

The region $\sigma \approx 2.73$ is where discrepancies between the present method and piston theory would be expected. Piston theory predicts that the steady state is reached as soon as the whole wing is immersed in a uniform step gust. Thus in Figs.3 and 4 the broken curves from piston theory lie above those conditioned to equations (39), but the discrepancies are less than 10%. In accord with these asymptotic results, the values $k_i(2.73)$ for $M = 0.8$ lie below those for $M = 0.4$ while piston theory, the true limit as $M \to \infty$, indicates a reversal of this trend once supersonic speeds are reached. It is interesting to note that, for both lift and pitching moment, the curves with $M = 0.4$ and $M = 0.8$ intersect near $\sigma = 2.3$ or 2.4, so that in the lower range $\sigma < 2$ the trend with Mach number is progressive.

In the attempted calculations for smaller σ, the function $Q_1'(\bar{\nu})$ for large $\bar{\nu}$ plays an increasingly important rôle. The expedient of using piston theory to determine $Q_i'(\bar{\nu})$ with $\bar{\nu} \geqslant 4.345$ may appear to be quite promising

for $M = 0.8$ in section 3.2, but in the final paragraph of section 3.3 it becomes questionable not only for $M = 0.4$ but to a lesser extent for $M = 0.8$. The results from equation (35) in Table 3 show negative values of k_1 and k_2 at $\sigma = 0.25$, which are more persistent for pitching moment than for lift and more pronounced at the lower Mach number; indeed, k_2 appears to remain negative at $M = 0.4$ until $\bar{\nu} > 1.4$. The unlikely phenomenon of negative $k_1(\sigma)$ in Fig.3 is very slight for $M = 0.8$ and can practically be overlooked, but it is so marked for $M = 0.4$ that calculations for $\bar{\nu} < 1.5$ can probably be discounted. With reference to Fig.4, on the other hand, it will be argued that small regions of negative $k_2(\sigma)$ are at least plausible.

As remarked in section 2, there exists in Ref.8 a general formulation of the linear problem with arbitrary time-dependent loading, in which the range of travel of acoustic waves from the pressure disturbances is clearly represented. Numerical solutions that preserve this feature are difficult to realize, and the present method founders in this respect in so far as equation (19) is adopted for the load distribution. Thus, an exceedingly large number of chordwise terms would be needed to maintain an approximation to zero loading until such time as a disturbance is physically possible. By way of illustration, a formula analogous to equation (35) has been used to evaluate the local loading at a few points on the root chord when the gust penetration, $\sigma = 0.5$, corresponds to the negative minimum of $k_1(\sigma)$ as calculated for $M = 0.4$ in Fig.3. The approximate results for three chordwise locations are given in the following table.

Eqn. (20) with $y = 0$		$\ell(x,0)$ when $\sigma = 0.5$	
ϕ	$x/\bar{c}$	$M = 0.4$	$M = 0.8$
0.25π	0.355	3.5	4.5
0.50π	0.863	-3.0	1.1
0.75π	1.370	-3.1	-1.5

It is easily seen that $\ell(x,0)$ should vanish in the region

$$\left.\begin{aligned} \frac{x}{\bar{c}} > \frac{\sigma}{M} &= 1.250 \quad \text{when} \quad M = 0.4 \\ &= 0.625 \quad \text{when} \quad M = 0.8 \end{aligned}\right\} \tag{40}$$

beyond the limit of disturbances propagated from the origin at the instant $\sigma = 0$. For $M = 0.4$, negative loading in the range

$$\sigma = 0.5 < \frac{x}{\bar{c}} < 1.250$$

is possible, but the large negative value at $x/\bar{c} = 1.370$ is quite unrealistic and doubtless provides an important contribution to the negative $k_1(\sigma)$. However, a moderate negative value of $\ell(x,0)$ at $x/\bar{c} = 0.863$ might be expected to arise from positive downwash induced aft of the gust front. By contrast, when $M = 0.8$ such downwash is restricted to the small region

$$0.5 < \frac{x}{\bar{c}} < 0.625 \quad ,$$

and the total contribution to $k_1(0.5)$ from the loading further aft would appear to be reasonably small, if not correctly zero. At all events, the few tabulated values of $\ell(x,0)$ are compatible with $k_1(0.5)$ as shown in Fig.3 and do not allay suspicion of the result for $M = 0.4$. With regard to the negative values in Fig.4, $k_2(\sigma)$ would be expected to lie below the curve predicted by piston theory, partly because of negative loading induced between the gust front and the rearward envelope of acoustic disturbances from the wing, and partly because the loading ahead of the gust front does not reach its steady state instantaneously. Since piston theory gives $k_2(\sigma)$ proportional to σ^3 with zero gradient and curvature at $\sigma = 0$, the possibility of a small region of negative $k_2(\sigma)$ cannot be ruled out, but the true result would be difficult to establish.

As a further indication of the order of accuracy of the calculated $k_1(0.5)$, the upper limit of integration in equation (35) has been varied; the consequence of using the less reliable equation (36) has also been examined. From Fig.2 it appears that the difference function $Q_1'(\bar{\nu}) - \bar{Q}_1'(\bar{\nu})$ in equation (35) is trivial when $\bar{\nu} \geqslant 4.345 (f \geqslant 6)$ and $M = 0.8$. At $M = 0.4$, however, there are pertinent differences between the calculated oscillatory lift from the present method and piston theory, and we obtain the following results.

Upper limit of integration	Values of $k_1(0.5)$ for $M = 0.4$	
	Equation (35)	Equation (36)
$f = 6$	-0.106	+0.171
$f = 7$	-0.072	+0.163

The excessive positive values from equation (36) must be rejected like the corresponding result $k_1(0) = 0.300$ discussed at the end of section 3.3. Even though the calculations from both equations (35) and (36) are consistent in predicting $dk_1/d\sigma < 0$, this result is unconvincing, because the gust is expected to produce a positive rate of growth of lift. The only glimmer of success in the above table for $\sigma = 0.5$ is the improvement with the longer range of integration in equation (35), which suggests a preference for the unconverged results from lifting-surface theory in the range $4.345 < \bar{\nu} < 6.196$ rather than those from piston theory for $M = 0.4$. However, once the wing is immersed in the gust $(\sigma > 2.73)$, the magnitude of the change in $k_1(\sigma)$ due to the increase in the range of integration falls below 0.01 and, even for $M = 0.4$, the present calculations are validated by equation (39).

We may conclude that in the range $0 < \sigma < 1.5$ the functions $k_1(\sigma)$ and $k_2(\sigma)$ should lie somewhere between the curves from piston theory and the present method. Above $\sigma = 1.5$, when about half the wing is immersed in the gust, the functions should be approaching the latter curves, which seem to be adequate for all practical purposes in the upper range $\sigma > 2$. This interpretation of the present method presumes that the flow is sufficiently compressible. The relative success of the calculations at $M = 0.8$ as opposed to $M = 0.4$ implies that the influence of the upper range of $\bar{\nu}$ (> 4.345) diminishes as Mach number increases; the same is true as gust penetration increases. The truncated upper limit of integration in equation (35) should probably satisfy some condition $M\sigma\bar{\nu} > 4$, say, on the frequency parameter based on penetration distance and the speed of sound. Thus the present method would suffice for $\sigma > 1/M$, while for very small σ piston theory might be the more reliable guide to the Küssner functions for lift and pitching moment.

The foregoing discussion relates to subsonic compressible flow and to swept wings of high aspect ratio, such that the streamwise length of planform is large relative to the geometric mean chord. In the lifting-surface calculations

the difficulties of numerical convergence for high $\bar{\nu}$ are aggravated by the need for large numbers of spanwise, as well as chordwise, terms; all three parameters (N,m,a) need to be fairly large (section 3.1). Let us compare the situation with that for wings of low aspect ratio in incompressible flow, and in particular for the planform considered by Mitchell in Fig.1a of Ref.9. In Fig.4 of Ref.9, he establishes consistent results for $k_i(\sigma)$ from the sine and cosine transforms corresponding to the present equations (15) and (16) and thus satisfies the identity (37) well enough. Moreover, there is no suggestion of negative $k_i(\sigma)$; on the contrary, the initial growth of lift in Fig.5 of Ref.9 is far in excess of the ratio $k_1(\sigma)$ that would be predicted by piston theory and relatively close to the result according to slender-wing theory

$$k_1(\sigma) = \left[\frac{s(\sigma)}{s}\right]^2 , \tag{41}$$

where $s(\sigma)$ denotes the local semi-span at the gust front. Although the infinite rate of travel of acoustic disturbances might suggest a greater susceptibility to negative lift aft of the gust front, this effect is precluded by the principles of slender-wing theory which must apply to a considerable degree. Likewise, the above assertion that the influence of the upper range of $\bar{\nu}$ increases as Mach number decreases may well be true for high aspect ratio, but untrue for low aspect ratio. By the inequalities (31) both low aspect ratio and low Mach number invalidate piston theory and its use in the present method, which cannot be relevant to the example considered by Mitchell. By the inequalities (29), on the other hand, there are weaker restrictions on the parameters m and a required in the lifting-surface method of Ref.5, and for moderately low aspect ratio this can probably be applied up to a frequency parameter at which it is safe, as Mitchell did, to truncate the range of integration in equation (15). There seems to be no reason why, under linear conditions, the influence of compressibility should not ease calculations for low and high aspect ratio alike.

4.2 Normal ramp gust

Consider a stationary ramp gust with gradient distance $\lambda_g \bar{c}$, as sketched in Fig.1b. In the special case $\psi = 0$ the boundary condition in place of equation (3) is

$$\left.\begin{aligned} w &= w_g && x \leqslant (\sigma - \lambda_g)\bar{c} \\ w &= \frac{w_g}{\lambda_g}\left(\sigma - \frac{x}{\bar{c}}\right) && (\sigma - \lambda_g)\bar{c} \leqslant x \leqslant \sigma\bar{c} \\ w &= 0 && \sigma\bar{c} \leqslant x \end{aligned}\right\} \quad . \quad (42)$$

This contributes a succession of identical elementary step gusts of velocity

$$\frac{w_g}{\lambda_g}\frac{\delta x}{\bar{c}} = \frac{w_g}{\lambda_g}\delta\xi$$

with delay times from $\xi\bar{c}/U = 0$ to $\lambda_g\bar{c}/U$. Thus the Küssner functions of section 4.1 can be generalized in the form

$$\left.\begin{aligned} k_i(\sigma,\lambda_g) &= \frac{1}{\lambda_g}\int_0^{\sigma} k_i(\sigma - \xi)d\xi && 0 \leqslant \sigma \leqslant \lambda_g \\ &= \frac{1}{\lambda_g}\int_0^{\lambda_g} k_i(\sigma - \xi)d\xi && \lambda_g \leqslant \sigma \end{aligned}\right\} \quad , \quad (43)$$

where $k_i(\sigma - \xi)$ is given in Table 3 or by equations (39) if $\sigma - \xi > 8$. More conveniently

$$\left.\begin{aligned} k_i(\sigma,\lambda_g) &= \frac{1}{\lambda_g}\int_0^{\sigma} k_i(\sigma')d\sigma' && 0 \leqslant \sigma \leqslant \lambda_g \\ &= \frac{1}{\lambda_g}\int_{\sigma-\lambda_g}^{\sigma} k_i(\sigma')d\sigma' && \lambda_g \leqslant \sigma \end{aligned}\right\} \quad , \quad (44)$$

where the integrals are evaluated by Simpson's rule from the knowledge of $k_i(\sigma')$ for $\sigma' = 0(0.25)8$ and by analytical integration over the range $8 \leqslant \sigma' \leqslant \sigma$, if necessary.

The functions $k_1(\sigma,\lambda_g)$ and $k_2(\sigma,\lambda_g)$ for lift and pitching moment about the root leading edge have been calculated for $M = 0.8$. The respective results in Tables 4 and 5 cover the range $\sigma \leqslant 16$ for nondimensional gradient lengths $\lambda_g = 2, 4, 6, 8, 12$ and 16. Alternative graphical presentations of

k_1 are found in Figs.5 and 6. If k_1 is plotted against σ, as in Fig.5, the limiting case of a step gust ($\lambda_g = 0$) from Fig.3 can be included; the effect of increasing λ_g is seen as a gradual flattening of the curve, so that it more nearly approaches the steady state $k_1 = 1$ at the instant $\sigma = \lambda_g + 2.73$ when the whole wing has traversed the ramp. The curves against σ/λ_g in Fig.6 emphasize the other limiting case $\lambda_g = \infty$, when the lift ratio has the same shape as the ramp. The growth of lift in the early stages can now be calculated with greater confidence, and the present results could easily be extended to gusts of arbitrary profile and finite length.

It is interesting to present results in the form of a transient pitching moment about the aerodynamic centre. The respective pitching axes

$$\frac{x_0}{\bar{c}} = \frac{x_{ac}}{\bar{c}} = -\frac{C_{m\infty}}{C_{L\infty}} = \frac{Q_2(0)}{Q_1(0)} \tag{45}$$

from the present method at $M = 0.4$ and 0.8 and from piston theory are given in Table 2. In accord with the definitions in equations (32),

$$\frac{C_m}{C_{L\infty}} = \frac{x_{ac}}{\bar{c}} [k_1(\sigma) - k_2(\sigma)] \tag{46}$$

is calculated from Table 3 for a step gust and plotted against σ in Fig.7a. The result for $M = 0.4$ is discredited, though there may be some substance in the delayed maximum at $\sigma = 1.8$. The virtual disappearance of $C_m/C_{L\infty}$ at $\sigma = 2.73$ is a consequence of equation (38), as remarked below it. Hence piston theory gives the right qualitative picture in Fig.7a and predicts the maximum value for $M = 0.8$ within 12%. The other curve in Fig.7a illustrates the smaller maximum in the case of a ramp gust. Even for the fairly steep ramp $\lambda_g = 2$ the maximum $\Delta C_m/C_{L\infty}$ has fallen by 32%. For longer ramps the maximum is replaced by a plateau of height inversely proportional to λ_g. This phenomenon in Fig.7b would be correctly predicted by piston theory, since in the range $2.73 < \sigma < \lambda_g$ the downwash from equation (42) is not only proportional to $1/\lambda_g$, but its rate of growth is uniform over the whole wing.

4.3 Oblique step gust

The derivation of the equations in section 2 serves to indicate that there is no difficulty in principle in extending the present method to the more complicated case of an oblique step gust. The basic oscillatory problem of the

sinusoidal gust in equation (8) then involves two parameters, the wavelength $2\pi\bar{c}/\bar{\nu}$ and the inclination ψ as defined in Fig.1c. Even for a single non-zero value of ψ, the computing time for $Q_i(\bar{\nu})$ would be doubled, as for each value of $\bar{\nu}$ it would be necessary to run separate solutions for the symmetrical and antisymmetrical parts of w/U in the spanwise sense. Such calculations have not been attempted but, as mentioned in section 2, the most economical approach would probably involve the reverse-flow theorem.

In the absence of results for the oblique step gust by the present method, the relatively simple application of piston theory has been made; a suitable method of calculation is outlined in the appendix and discussed in section 3.2. Since piston theory has been shown to give fair predictions for normal gusts at $M = 0.8$ in Figs.3, 4 and 7a, the formulae (A-21) to (A-23) are likely to yield a useful indication of the behaviour of the lift, pitching moment and rolling moment. The normalized Küssner functions $k_1(\sigma)$ and $k_2(\sigma)$, the transient pitching moment about the aerodynamic centre and the transient rolling moment have been computed in Table 6 for four special values of $\tan\psi$, viz.,

$\tan\psi = 0.4107$, $\psi = \Lambda_t$, gust front parallel to trailing edge,

$\tan\psi = 0.7440$, $\psi = \Lambda_\ell$, gust front parallel to leading edge,

$\tan\psi = 0.9107$, root leading edge and tip trailing edge enter gust simultaneously,

$\tan\psi = 1.4107$, root leading edge and mid-trailing edge enter gust simultaneously.

The origin is taken at the root leading edge, so that it enters the gust when $\sigma = 0$. When $\psi = \Lambda_t$, the aerodynamic quantities show discontinuities in slope at $\sigma = 1.5$ when the whole starboard trailing edge enters the gust. Similarly, the calculated forces have non-zero slope at $\sigma = 0$ in the special case $\psi = \Lambda_\ell$ when the gust front coincides with the starboard leading edge. For larger ψ, the gust strikes the wing tip first at the instant

$$\sigma = -3(\tan\psi - \tan\psi_\ell) \quad . \tag{47}$$

It is clear from equations (A-17) to (A-20) of the appendix that the lift is quadratic and both moments are cubic in σ, and that each polynomial function

collocation method to deal with sinusoidal gusts of very small wavelength. In view of restrictions on the number of chordwise terms, it becomes difficult to calculate the wing loading after only small penetration into the step gust. Piston theory is applicable in compressible flow when the frequency parameter is very high, and the consequences of replacing subsonic lifting-surface theory by piston theory in an upper frequency range are most instructive.

(3) The above procedure has been adopted in equation (35), which has been applied to a normal step gust for Mach numbers 0.4 and 0.8 with reasonable success in the latter case. The relative failure at the lower Mach number appears to be associated partly with the unsuitability of piston theory when compressibility is slight, and partly with the greater importance of the higher frequencies at lower speeds. It appears that the reciprocal of the frequency parameter based on penetration distance and the speed of sound may provide a measure of the influence of a particular frequency on the Küssner functions.

(4) The lift and nose-down pitching moment about the leading apex are calculated to be negative for small penetration distances, more persistently in the case of pitching moment and the lower Mach number. While the phenomenon of negative lift is discredited, it is considered plausible, but unsubstantiated, that in subsonic compressible flow the downwash aft of the gust front could induce negative loading compatible with a nose-up pitching moment on a wing of high aspect ratio in the early stages of gust entry.

(5) The present method gives good correlation with the known asymptotic behaviour in equation (38) at large time as the steady state is approached. This restores confidence in the calculations at the lower Mach number once most of the wing is immersed in the gust. An interesting corollary to equation (38) is that the transient pitching moment about the aerodynamic centre disappears inversely as the cube of the distance travelled, although in practice this would be obscured by aircraft response and there would be a corresponding delay in approaching steady lift.

(6) The present method is at a disadvantage when the aspect ratio is high, because large numbers of spanwise, as well as chordwise, terms are needed. Provided that they are presented in suitable nondimensional form, calculations by piston theory alone may well be reliable within 10 or 20%. It is recommended that the proportional growth of aerodynamic force should be taken between the results of piston theory and the present method for small penetration distances, should approach the latter result before the wing is completely immersed in the

gust and should follow the correct asymptotic behaviour soon after this condition is reached.

(7) The alternative cosine transform of equation (16) or (36) has proved to be remarkably unsuccessful at small penetration distances, primarily because it does not automatically vanish at the instant when the wing first meets the gust. This necessary condition yields the identity in equation (37), which can be regarded as an ultimate challenge to a general numerical technique of solving oscillatory linear problems in subsonic flow. While the infinite integral (37) converges rapidly to unity by means of piston theory, its inferred slow convergence from lifting-surface theory suggests that the two theories are much slower to coalesce at high frequency than is anticipated in the use of equation (35) or (36).

(8) Rigorous justification of the present method for small as well as large distances of penetration would demand overlapping lower and upper ranges of frequency parameter where respectively the lifting-surface method and piston theory apply. The failure to satisfy equation (37) implies a gap between these ranges, which can only be bridged by more elaborate collocation solutions over a substantial range of high frequency parameter. To extend the investigation in this respect, or in range of planform, would be justified if there were sufficient uncertainty in the prediction of aircraft response to a known vertical gust due to approximations in the unsteady aerodynamic input.

(9) Although a lifting-surface method may cope satisfactorily with a given oscillatory downwash distribution, it may not be ideally suited to the calculation of loads resulting from a vertical gust. Through the assumption of the finite summation in equation (19) the present method implies non-zero loading over all regions of the planform, even before it is physically possible for acoustic waves to travel from the intersection of the wing and the gust front. The calculated negative lift at small time includes a contribution from impossible negative loads aft of all acoustic disturbances. This feature of a collocation method is especially hard to eradicate, but the integral equations for doing so exist in Ref.8.

(10) There is no difficulty in principle in extending the present method from a normal step gust to an oblique gust of arbitrary profile and length. All that has been done in this respect is to derive results for a normal ramp gust in section 4.2. Unless the ramp is steep, the transient pitching moment about the aerodynamic centre exhibits the plateau behaviour in Fig.7, which would also be predicted by piston theory.

(11) Some qualitative results for an oblique step gust have been calculated by piston theory alone and discussed in section 4.3. The rapid initial growth of lift and the possible occurrence of negative pitching moment about the aerodynamic centre are primarily associated with the sweepback of the planform. The large maximum rolling moment for moderately small inclination of the gust front illustrates the importance of the lateral aerodynamic characteristics of a wing in a vertical gust.

Acknowledgements

The author wishes to acknowledge that Miss Doris Lehrian assisted with the planning of the calculations and that Mrs. Sylvia Lucas was responsible for most of the computations and diagrams.

Appendix

GUST FUNCTIONS FROM PISTON THEORY

Piston theory provides a simple method for the evaluation of wing loading in unsteady conditions. Its numerous applications to high-speed flow have been discussed by Ashley and Zartarian[11]. In the context of linear theory we only need to consider the small-disturbance relation for the loading

$$\frac{\Delta p}{\frac{1}{2}\rho U^2} = -\frac{4w(t)}{MU} \quad , \tag{A-1}$$

where $w(t)$ is the local upward velocity of the wing with arbitrary time-dependence. It is clear from section 1.4 of Ref.12, that under oscillatory conditions equation (A-1) is subject to the severe restrictions

$$\left.\begin{aligned} \bar{\nu}M &\gg 1 \\ A\bar{\nu}M &\gg 1 \end{aligned}\right\} \quad . \tag{A-2}$$

Nevertheless, unless the flow is incompressible, there is an upper range of frequency parameter for which piston theory becomes available. The second condition is more readily satisfied for the wing of high aspect ratio to be considered.

For a sinusoidal gust we consider the equivalent wing motion

$$w(x,t) = \text{real part of } -U \exp\left(i\omega t + \frac{i\omega x}{U}\right) \quad . \tag{A-3}$$

As usual, the harmonic time-dependence factor $e^{i\omega t}$ is omitted and equation (A-1) is combined with

$$w = -Ue^{i\bar{\nu}\xi} \quad , \tag{A-4}$$

where $\bar{\nu} = \omega\bar{c}/U$ and $\xi = x/\bar{c}$. The corresponding nondimensional complex lift is simply

$$Q_1(\bar{\nu}) = \frac{1}{S}\iint_S \frac{\Delta p}{\rho U^2}\, dS = \frac{1}{M}\iint_S e^{i\bar{\nu}\xi} d\xi d\eta \quad . \tag{A-5}$$

The area of the particular planform in Fig.1a is defined by

$$\left.\begin{aligned} 0 \leqslant |\eta| &\leqslant \frac{\xi}{\sqrt{3}+0.5} && (0 \leqslant \xi \leqslant 1.5) \\ \frac{\xi-1.5}{\sqrt{3}-0.5} \leqslant |\eta| &\leqslant \frac{\xi}{\sqrt{3}+0.5} && (1.5 \leqslant \xi \leqslant \sqrt{3}+0.5) \\ \frac{\xi-1.5}{\sqrt{3}-0.5} \leqslant |\eta| &\leqslant 1 && (\sqrt{3}+0.5 \leqslant \xi \leqslant \sqrt{3}+1) \end{aligned}\right\}, \quad \text{(A-6)}$$

and it follows that

$$Q_1(\bar{\nu}) = \frac{2}{M\bar{\nu}^2}\left[\frac{e^{i\bar{\nu}(1.5)} - e^{i\bar{\nu}(\sqrt{3}+1)}}{\sqrt{3}-0.5} - \frac{1 - e^{i\bar{\nu}(\sqrt{3}+0.5)}}{\sqrt{3}+0.5}\right] . \quad \text{(A-7)}$$

Similarly the complex pitching moment is represented by

$$Q_2(\bar{\nu}) = \frac{1}{S}\iint_S \left(\frac{x - x_0}{\bar{c}}\right)\frac{\Delta p}{\rho U^2}\, dS = \frac{1}{M}\iint_S \left(\xi - \frac{x_0}{\bar{c}}\right)e^{i\bar{\nu}\xi} d\xi d\eta \quad \text{(A-8)}$$

$$= -\frac{x_0}{\bar{c}} Q_1 + \frac{2i}{\bar{\nu}} Q_1 + \frac{2}{M\bar{\nu}^2}\left[e^{i\bar{\nu}(\sqrt{3}+0.5)} + \frac{1.5e^{i\bar{\nu}(1.5)} - (\sqrt{3}+1)e^{i\bar{\nu}(\sqrt{3}+1)}}{\sqrt{3}-0.5}\right]. \quad \text{(A-9)}$$

The real and imaginary parts of Q_1 from equation (A-7) are included in Table 1, while the real part of Q_2 is given in Table 2 both for $x_0 = 0$ and for the pitching axis through the aerodynamic centre

$$\frac{x_0}{\bar{c}} = \frac{Q_2(0)}{Q_1(0)} = \frac{3}{4} + \frac{5}{12}\sqrt{3} = 1.4717 . \quad \text{(A-10)}$$

The results are expected to become reliable when $\bar{\nu}$ is much larger than $1/M$. Little confidence can be placed in equation (A-10), however, since there is no justification for piston theory in steady flow.

A normal step gust can be built up by superposition, and the growth of lift or pitching moment can be formulated from equation (11) or (12) together with equation (A-7) or (A-9). Exact integration leads to different polynomial expressions for $k_1(\sigma)$ and $k_2(\sigma)$ according to the range of σ. A simpler derivation is to set

$$\left.\begin{aligned} \frac{\Delta p}{\rho U^2} &= \frac{2w_g}{MU} && 0 \leqslant \xi < \sigma \\ &= 0 && \xi > \sigma \end{aligned}\right\} \qquad \text{(A-11)}$$

in equations (A-5) and (A-8) to give $Q_{1g}(\sigma)$ and $Q_{2g}(\sigma)$. Hence

$$k_1(\sigma) = \frac{Q_{1g}(\sigma)}{Q_1(0)} \begin{cases} = 0 & (\sigma \leqslant 0) \\ = 0.22401\sigma^2 & (0 \leqslant \sigma \leqslant 1.5) \\ = 0.22401\sigma^2 - 0.40583(\sigma - 1.5)^2 & (1.5 \leqslant \sigma \leqslant 2.23205) \\ = -0.40583\sigma^2 + 2.21748\sigma - 2.02914 & (2.23205 \leqslant \sigma \leqslant 2.73205) \\ = 1 & (\sigma \geqslant 2.73205) \end{cases} \qquad \text{(A-12)}$$

Similarly for the axis $x_0 = 0$

$$k_2(\sigma) = \frac{Q_{2g}(\sigma)}{Q_2(0)} \begin{cases} = 0 & (\sigma \leqslant 0) \\ = 0.10148\sigma^3 & (0 \leqslant \sigma \leqslant 1.5) \\ = -0.08236\sigma^3 + 0.41364\sigma^2 - 0.31023 & (1.5 \leqslant \sigma \leqslant 2.23205) \\ = -0.18384\sigma^3 + 0.75338\sigma^2 - 0.87444 & (2.23205 \leqslant \sigma \leqslant 2.73205) \\ = 1 & (\sigma \geqslant 2.73205) \end{cases} \qquad \text{(A-13)}$$

Numerical results from equations (A-12) and (A-13) appear in the last two columns of Table 3 and are independent of Mach number. Such results would be valid in high supersonic flight, but for subsonic speeds they should be regarded as approximations to be used when nothing better is available.

Similarly, piston theory provides rough approximations to aerodynamic forces from oblique entry into a stationary step gust; more accurate results would be exceedingly tedious to obtain. Following the pattern of equations (A-12) and (A-13), the lift is quadratic in σ while the pitching and rolling moments are cubic in σ, and their formulae change whenever a vertex of the planform enters the gust. Let ψ denote the inclination of the transverse axis $y = 0$ to the gust front (Fig.1c). Then the following numerical procedure is recommended.

(1) Evaluate and place in increasing order the quantities

$$0 \quad , \quad c_R \cos\psi \quad , \quad x_{\ell T} \pm s \sin\psi \quad , \quad (x_{\ell T} + c_T)\cos\psi \pm s \sin\psi \quad ,$$

the normal distances from each of the six vertices to the gust front at $\sigma = 0$ as it passes the origin (Fig.1a). Label them

$$h_n = \sigma_n \bar{c} \cos\psi \qquad (n = 1,2,\ldots 6) \; . \quad \text{(A-14)}$$

(2) Consider each strip $\sigma_n \leqslant \sigma \leqslant \sigma_{n+1}$ as traversed by the gust. It contains a trapezium of planform with vertices

$$(x_{n1},y_{n1}) \quad , \quad (x_{n2},y_{n2}) \quad , \quad (x_{n+1,1},y_{n+1,1}) \quad , \quad (x_{n+1,2},y_{n+1,2}) \quad ;$$

because of the reflex angle at $(c_R,0)$ a second trapezium can appear when $0 \leqslant \psi < \Lambda_t$, the angle of sweepback of the trailing edge. Then calculate

$$\left.\begin{aligned} h_{n+1} - h_n &= (x_{n+1,1} - x_{n1})\cos\psi - (y_{n+1,1} - y_{n1})\sin\psi \\ &= (x_{n+1,2} - x_{n2})\cos\psi - (y_{n+1,2} - y_{n2})\sin\psi \end{aligned}\right\} \; . \quad \text{(A-15)}$$

With the gust front at

$$\sigma = (1 - \lambda)\sigma_n + \lambda\sigma_{n+1} \qquad (0 \leqslant \lambda \leqslant 1) \qquad \text{(A-16)}$$

evaluate the length of strip

$$\left.\begin{aligned} \ell &= (1 - \lambda)\ell_n + \lambda\ell_{n+1} \\ \text{where for each } n \quad & \\ \ell_n &= (x_{n2} - x_{n1})\,\mathrm{cosec}\,\psi = (y_{n2} - y_{n1})\sec\psi \end{aligned}\right\} \; . \quad \text{(A-17)}$$

(3) Evaluate the contributions to lift, pitching moment $(x_0 = 0)$ and rolling moment from the region between σ_n and σ in the respective formulae

$$\frac{\delta C_L}{C_{L\infty}} = \frac{\lambda(h_{n+1} - h_n)}{2S}\,[\ell_n + \ell] \quad , \tag{A-18}$$

$$\frac{\delta C_m}{C_{L\infty}} = -\frac{\lambda(h_{n+1} - h_n)}{2S\bar{c}}\left[\tfrac{1}{2}(x_{n1} + x_{n2})(\ell_n + \ell) + \frac{1}{6}\lambda(x_{n+1,1} + x_{n+1,2} - x_{n1} - x_{n2})(\ell_n + 2\ell)\right] \tag{A-19}$$

and

$$\frac{\delta C_\ell}{C_{L\infty}} = -\frac{\lambda(h_{n+1} - h_n)}{4Ss}\left[\tfrac{1}{2}(y_{n1} + y_{n2})(\ell_n + \ell) + \frac{1}{6}\lambda(y_{n+1,1} + y_{n+1,2} - y_{n1} - y_{n2})(\ell_n + 2\ell)\right] \quad , \tag{A-20}$$

where $C_{L\infty} = 2Q_1(0)$ is the final lift coefficient.

(4) Substitute $\lambda = 1$ in equations (A-18) to (A-20) to deal with the complete strips and calculate

$$k_1(\sigma) = \frac{C_L}{C_{L\infty}} = \sum_{u=1}^{n-1} \frac{h_{u+1} - h_u}{2S}\,[\ell_u + \ell_{u+1}] + \frac{\delta C_L}{C_{L\infty}} \quad , \tag{A-21}$$

$$\frac{C_m}{C_{L\infty}} = \frac{x_0}{\bar{c}}\,k_1(\sigma) + \frac{\delta C_m}{C_{L\infty}} - \sum_{u=1}^{n-1} \frac{h_{u+1} - h_u}{12S\bar{c}}\,[(x_{u1} + x_{u2})(2\ell_u + \ell_{u+1}) + (x_{u+1,1} + x_{u+1,2})(\ell_u + 2\ell_{u+1})] \tag{A-22}$$

and

$$\frac{C_\ell}{C_{L\infty}} = \frac{\delta C_\ell}{C_{L\infty}} - \sum_{u=1}^{n-1} \frac{h_{u+1} - h_u}{24Ss}\,[(y_{u1} + y_{u2})(2\ell_u + \ell_{u+1}) + (y_{u+1,1} + y_{u+1,2})(\ell_u + 2\ell_{u+1})] \quad . \tag{A-23}$$

Although this general procedure applies to an arbitrary straight-tapered swept wing and to any inclination of the gust front, the first two stages vary considerably according to the geometry. Naturally the number of strips will be reduced when two vertices enter the gust simultaneously. The illustrative

values in Table 6 are not sufficient to define the curves against σ, because each change of interval $\sigma_n < \sigma < \sigma_{n+1}$ introduces discontinuities in curvature. Moreover, there can be sudden changes of slope when an edge of the planform coincides with the gust front. The quantities from equations (A-21) to (A-23) are plotted in Figs.8 to 10 for the planform of Fig.1a, and these results are discussed in section 4.3.

Table 1

COMPLEX LIFT Q_1 FROM A SINUSOIDAL GUST OF WAVELENGTH $2\pi\bar{c}/\bar{\nu}$

$\bar{\nu}$	Present theory M = 0.4	Present theory M = 0.8	Piston theory M = 0.8
0	2.0979 + i 0.0000	2.5505 + i 0.0000	2.5000 + i 0.0000
0.2484	1.8203 + i 0.7414	2.2255 + i 0.6627	2.3107 + i 0.8849
0.5000	1.1705 + i 1.3878	1.5915 + i 1.3647	1.7761 + i 1.6104
1.0257	-0.6414 + i 1.6289	-0.0312 + i 1.9127	0.1153 + i 2.0871
1.6085	-1.8120 + i 0.2473	-1.2496 + i 0.9746	-1.1629 + i 1.0795
2.2936	-1.0749 - i 1.3584	-0.9798 - i 0.3365	-0.8829 - i 0.3025
3.1569	0.3906 - i 1.0844	0.0384 - i 0.3352	0.1154 - i 0.2719
4.3451	0.2424 - i 0.1631	-0.0808 + i 0.0737	-0.0944 + i 0.0778
5.1516	0.0659 + i 0.0185	-0.0361 + i 0.0090	-0.0170 - i 0.0374
6.1957	-0.2405 + i 0.3374	-0.1632 + i 0.1483	-0.0545 + i 0.0843

Table 2

REAL PART OF PITCHING MOMENT $-Q_2'$ FROM SINUSOIDAL GUSTS

Theory	M	$x_{ac}/\bar{c}$
Present	0.4	1.2583
Present	0.8	1.2736
Piston	Any	1.4717

$\tilde{\nu}$	Present theory $x_0 = 0$		Present theory $x_0 = x_{ac}$		Piston theory M = 0.8	
	M = 0.4	M = 0.8	M = 0.4	M = 0.8	$x_0 = 0$	$x_0 = x_{ac}$
0	-2.6398	-3.2483	0	0	-3.6792	0
0.2484	-2.2248	-2.7522	+0.0657	+0.0823	-3.3294	+0.0713
0.5000	-1.2414	-1.7202	+0.2314	+0.3068	-2.3500	+0.2638
1.0257	+1.3577	+0.9110	+0.5506	+0.8712	+0.5720	+0.7417
1.6085	+2.4854	+2.4184	+0.2054	+0.8268	+2.4208	+0.7094
2.2936	+0.4797	+1.1232	-0.8729	-0.1248	+1.1547	-0.1447
3.1569	-1.3626	-0.6884	-0.8711	-0.6395	-0.7481	-0.5784
4.3451	+0.0787	+0.1648	+0.3837	+0.0619	+0.2319	+0.0930
5.1516	-0.0847	-0.0214	-0.0019	-0.0674	-0.0613	-0.0863
6.1957	+0.3302	+0.2022	+0.0275	-0.0056	+0.0363	-0.0439

Table 3

RATIO OF TRANSIENT TO FINAL LIFT AND PITCHING MOMENT ($x_0 = 0$)
AFTER NORMAL ENTRY INTO A STEP GUST

σ	Present theory M = 0.4		Present theory M = 0.8		Piston theory	
	k_1	k_2	k_1	k_2	k_1	k_2
0.25	-0.078	-0.027	-0.009	-0.030	0.014	0.002
0.50	-0.106	-0.054	0.014	-0.048	0.056	0.013
0.75	-0.096	-0.078	0.074	-0.040	0.126	0.043
1.0	-0.046	-0.092	0.168	0.004	0.224	0.101
1.5	0.234	0.036	0.447	0.235	0.504	0.342
2.0	0.636	0.431	0.732	0.590	0.795	0.685
2.5	0.941	0.909	0.912	0.890	0.978	0.962
3.0	0.964	0.965	0.939	0.938	1.000	1.000
4.0	0.976	0.971	0.955	0.956	1.000	1.000
6.0	0.987	0.985	0.980	0.980	1.000	1.000
8.0	0.994	0.994	0.990	0.990	1.000	1.000

Table 4

LIFT RATIO k_1 FROM A NORMAL GUST WITH RAMP LENGTH $\lambda_g \bar{c}$

σ	$\lambda_g = 2$	$\lambda_g = 4$	$\lambda_g = 6$	$\lambda_g = 8$	$\lambda_g = 12$	$\lambda_g = 16$
0	0	0	0	0	0	0
0.5	-0.001	0.000	0.000	0.000	0.000	0.000
1.0	0.019	0.009	0.006	0.005	0.003	0.002
1.5	0.094	0.047	0.031	0.023	0.016	0.012
2.0	0.242	0.121	0.081	0.061	0.040	0.030
2.5	0.452	0.226	0.150	0.113	0.075	0.056
3.0	0.665	0.342	0.228	0.171	0.114	0.086
4.0	0.916	0.579	0.386	0.289	0.193	0.145
5.0	0.955	0.810	0.546	0.410	0.273	0.205
6.0	0.969	0.942	0.709	0.532	0.354	0.266
7.0	0.980	0.967	0.867	0.655	0.436	0.327
8.0	0.986	0.978	0.957	0.778	0.519	0.389
10.0	0.992	0.989	0.983	0.966	0.684	0.513
12.0	0.995	0.994	0.991	0.986	0.850	0.638
16.0	0.997	0.997	0.996	0.995	0.989	0.887

Table 5

PITCHING MOMENT RATIO k_2 FROM A NORMAL GUST WITH RAMP LENGTH $\lambda_g \bar{c}$

σ	$\lambda_g = 2$	$\lambda_g = 4$	$\lambda_g = 8$	$\lambda_g = 16$
0	0	0	0	0
0.5	-0.007	-0.004	-0.002	-0.001
1.0	-0.016	-0.008	-0.004	-0.002
1.5	0.010	0.005	0.002	0.001
2.0	0.113	0.056	0.028	0.014
2.5	0.309	0.151	0.075	0.038
3.0	0.549	0.267	0.133	0.067
4.0	0.894	0.504	0.252	0.126
5.0	0.956	0.752	0.372	0.186
6.0	0.969	0.932	0.494	0.247
7.0	0.979	0.968	0.617	0.309
8.0	0.986	0.978	0.741	0.370
10.0	0.992	0.989	0.961	0.494
12.0	0.995	0.994	0.986	0.619
16.0	0.997	0.997	0.995	0.868

Table 6

LIFT AND PITCHING MOMENT RATIOS AND PITCHING AND ROLLING MOMENTS FROM OBLIQUE STEP GUSTS BY PISTON THEORY

$\tan \psi$	σ	k_1	k_2	$\frac{C_m}{C_{L\infty}}$	$\frac{C_\ell}{C_{L\infty}}$
	1.000	0.3222	0.2099	0.1652	-0.0382
	1.250	0.4878	0.4017	0.1267	-0.0661
0.4107	1.500	0.6624	0.5907	0.1055	-0.0924
($\psi = \Lambda_t$)	2.482	0.8468	0.7786	0.1003	-0.0576
	3.464	0.9746	0.9572	0.0256	-0.0118
	3.964	1.0000	1.0000	0.0000	0.0000
	0.250	0.1285	0.1057	0.0335	-0.0312
	0.500	0.2640	0.2344	0.0435	-0.0622
0.7440	1.500	0.6260	0.5642	0.0909	-0.0971
($\psi = \Lambda_\ell$)	2.982	0.8395	0.7708	0.1010	-0.0600
	4.464	0.9820	0.9693	0.0187	-0.0086
	4.964	1.0000	1.0000	0.0000	0.0000
	0	0.1250	0.1405	-0.0229	-0.0417
	0.750	0.4346	0.4143	0.0299	-0.0956
0.9107	1.500	0.6133	0.5558	0.0846	-0.0985
	3.232	0.8369	0.7682	0.1011	-0.0609
	4.964	0.9842	0.9731	0.0164	-0.0076
	5.464	1.0000	1.0000	0.0000	0.0000
	-1.500	0.0312	0.0470	-0.0232	-0.0143
	0	0.3125	0.3464	-0.0499	-0.0885
1.4107	1.500	0.5870	0.5398	0.0695	-0.1008
	3.982	0.8314	0.7626	0.1012	-0.0625
	6.464	0.9886	0.9804	0.0121	-0.0055
	6.964	1.0000	1.0000	0.0000	0.0000

SYMBOLS

a	spanwise integration parameter in equation (26)
A	aspect ratio of planform; $2s/\bar{c}$
$c(y)$	local chord
$\bar{c}$	geometric mean chord; $S/2s$
c_R, c_T	root chord, tip chord
C_ℓ	rolling moment coefficient in equation (32)
C_L, $C_{L\infty}$	lift/$(\frac{1}{2}\rho U^2 S)$, its steady-state value
C_m, $C_{m\infty}$	nose-up pitching moment/$(\frac{1}{2}\rho U^2 S\bar{c})$, its steady-state value
f	auxiliary frequency parameter in equation (30)
h_n	initial location of planform vertices $(n = 1,2,...6)$ normal to gust front
$k_i(\sigma)$	growth of lift $(i = 1)$ or pitching moment $(i = 2)$ in equation (15)
$\bar{k}_i(\sigma)$	$k_i(\sigma)$ from piston theory (where the distinction is necessary)
$\ell(x,y)$	lift per unit area/$(\frac{1}{2}\rho U^2)$
ℓ, ℓ_n	length of strip where gust front intersects planform
m	number of collocation sections
M	Mach number of flight
N	number of chordwise functions in equation (19)
$Q_i(\bar{\nu})$	generalized force $(i = 1,2)$ due to sinusoidal gust; $Q_i'(\bar{\nu}) + iQ_i''(\bar{\nu})$
$\bar{Q}_i(\bar{\nu})$	$Q_i(\bar{\nu})$ from piston theory (where the distinction is necessary)
Q_{ig}	generalized force due to step gust normalized as in equation (18)
s	semi-span of wing
S	area of planform
t	time
U	velocity of flight
w	upwash velocity
$\bar{w}$	modified complex upwash in equation (25)
w_g	velocity of uniform up-gust
W	upwash velocity due to a sinusoidal gust
x	distance aft of the origin (Fig.1a)
x_0	location of pitching axis

SYMBOLS (concluded)

x_{ac}	location of aerodynamic centre in equation (45)
$x_{\ell}(y)$	ordinate of leading edge
$x_{\ell T}$	ordinate of tip leading edge; $x_{\ell}(s)$
x_{n1}, x_{n2}	ordinate of points where gust front ($\sigma = \sigma_n$) intersects planform
$x_{p\nu}$	ordinate of collocation point in equation (28) ($p = 1,2,...N$)
y	distance to starboard (Fig.1a)
y_{n1}, y_{n2}	ordinate of points where gust front ($\sigma = \sigma_n$) intersects planform
y_r	location of loading section in equation (22) ($r = 1,2,...m$)
y_{ν}	location of collocation section in equation (28) ($\nu = 1,2,...m$)
z	distance upwards (Fig.1b)
$z_{\iota}(x,y)$	force modes ($\iota = 1,2$) in equations (24)
Γ_q, Γ_{qr}	loading coefficients in equations (19) and (21)
δC_L	contribution to C_L in equation (A-18); similarly δC_{ℓ}, δC_m
Δp	lift per unit area
η	spanwise ordinate y/s
θ, θ_r	angular spanwise parameter in equation (23), (22)
λ	auxiliary variable for σ in equation (A-16)
λ_g	gust gradient distance as a fraction of $\bar{c}$
Λ_{ℓ}, Λ_t	angle of sweepback of leading edge, trailing edge
$\bar{\nu}$	frequency parameter $\omega\bar{c}/U$
$\bar{\nu}_f$	particular value of $\bar{\nu}$ associated with the variable f
ξ	chordwise variable $x/\bar{c}$
ρ	density of air
σ	location of gust front; nondimensional time $Ut/\bar{c}$
σ_n	ordered values of σ when planform vertex enters gust ($n = 1,2,...6$)
σ, τ	indices of polynomial $\xi^{\sigma}\eta^{\tau}$ representative of oscillatory mode
ϕ, ϕ_p	angular chordwise parameter in equation (20), (28)
ψ	inclination of gust front to plane x = constant (Fig.1c)
ω	circular frequency of oscillation

REFERENCES

No.	Author	Title, etc.
1	H.G. Kussner	Zusammenfassender Bericht über den instationären Auftrieb von Flügeln. Luftfahrtforschung Bd. 13, pp.410-424 (1936)
2	H. Lomax	Indicial aerodynamics. Manual on Aeroelasticity, Vol.2, Ch.6 AGARD (ed., W.P. Jones) (1960)
3	C.G.B. Mitchell	Calculation of the response of a flexible aircraft to harmonic and discrete gusts by a transform method. ARC R&M 3498 (1965)
4	C.G.B. Mitchell	Computer programmes to calculate the response of flexible aircraft to gusts and control movements. ARC CP 957 (1966)
5	Doris E. Lehrian H.C. Garner	Theoretical calculation of generalized forces and load distribution on wings oscillating at general frequency in a subsonic stream. ARC R&M 3710 (1971)
6	J.A. Drischler	Calculation and compilation of the unsteady-lift functions for a rigid wing subjected to sinusoidal gusts and to sinusoidal sinking oscillations. NACA Technical Note 3748 (1956)
7	J.A. Drischler F.W. Diederich	Lift and moment responses to penetration of sharp-edged travelling gusts,with application to penetration of weak blast waves. NACA Technical Note 3956 (1957)
8	J.A. Drischler	An integral equation relating the general time-dependent lift and downwash distributions on finite wings in subsonic flow. NASA Technical Note D-1521 (1963)
9	C.G.B. Mitchell	The calculation of aerodynamic forces and pressures on wings entering step gusts. RAE Technical Report 67054 (ARC 29462) (1967) Aeronaut. J. Vol.72, pp.535-539 (1968)

REFERENCES (concluded)

No.	Author	Title, etc.
10	H.N. Murrow K.G. Pratt J.A. Drischler	An application of a numerical technique to lifting-surface theory for calculation of unsteady aerodynamic forces due to continuous sinusoidal gusts on several wing planforms at subsonic speeds. NASA Technical Note D-1501 (1963)
11	H. Ashley G. Zartarian	Piston theory - A new aerodynamic tool for the aeroelastician. J. Aeronaut. Sci. Vol.23, pp.1109-1118 (1956)
12	J.W. Miles	The potential theory of unsteady supersonic flow. Cambridge University Press (1959)
13	H.C. Garner R.D. Milne	Asymptotic expansion for transient forces from quasi-steady subsonic wing theory. Aeronaut. Q. Vol.XVII, pp.343-350 (1966)

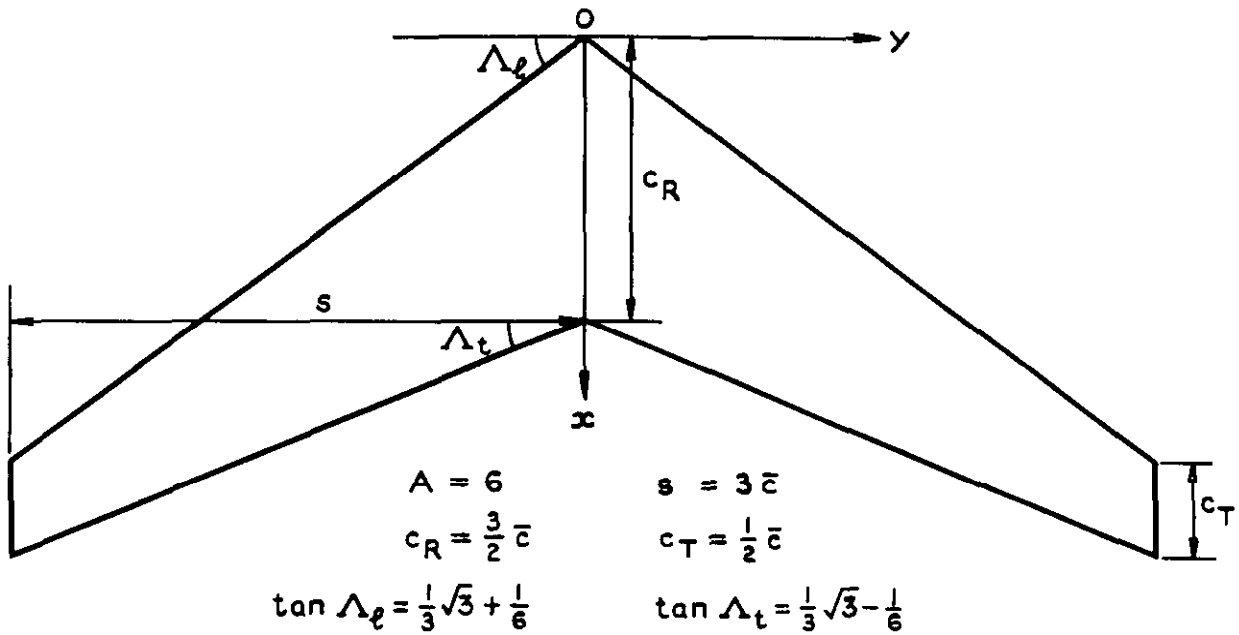

$A = 6$ $\quad s = 3\bar{c}$

$c_R = \frac{3}{2}\bar{c}$ $\quad c_T = \frac{1}{2}\bar{c}$

$\tan \Lambda_\ell = \frac{1}{3}\sqrt{3} + \frac{1}{6}$ $\quad \tan \Lambda_t = \frac{1}{3}\sqrt{3} - \frac{1}{6}$

a Planform of wing

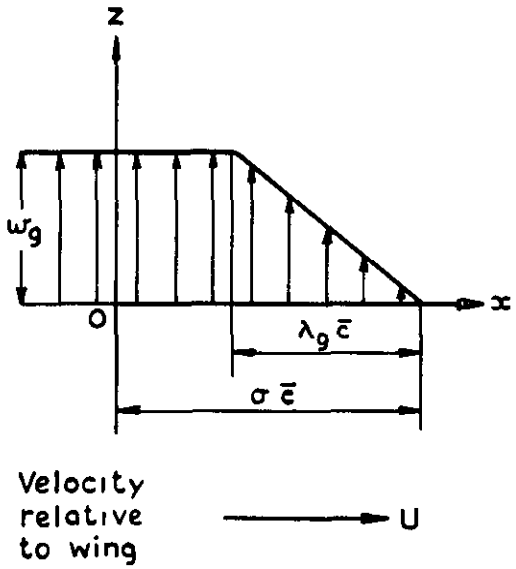

b Normal ramp gust

$\psi = 0$

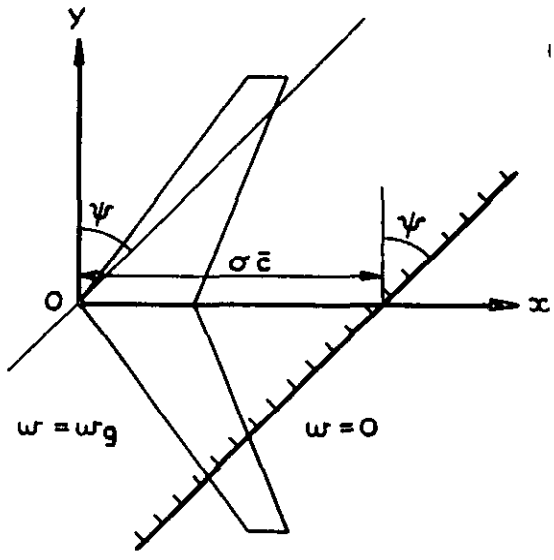

c Oblique step gust

$\lambda_g = 0$

Fig.1a-c Geometry of planform and vertical gust

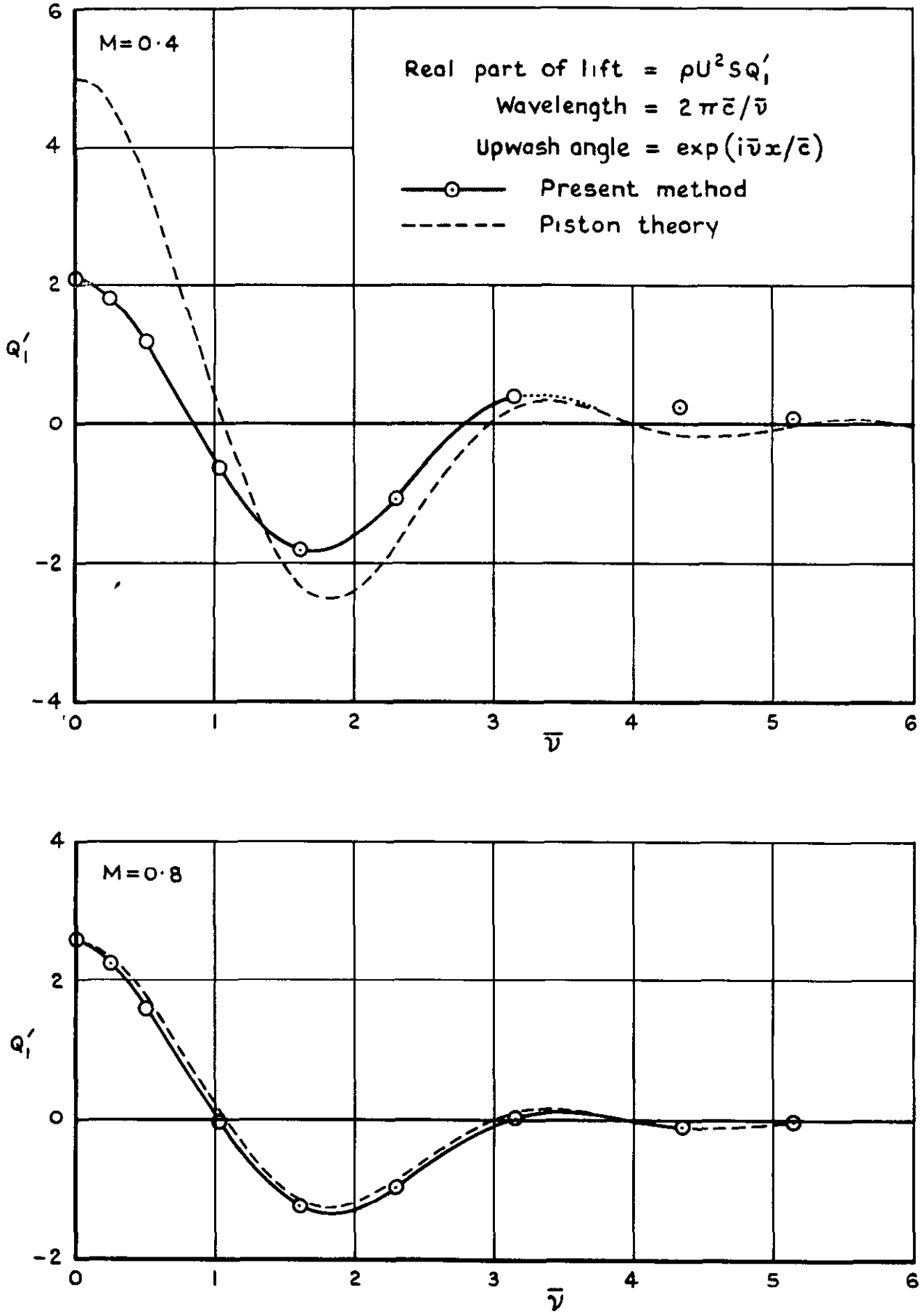

Fig.2 Lift from sinusoidal gusts of variable wavelength

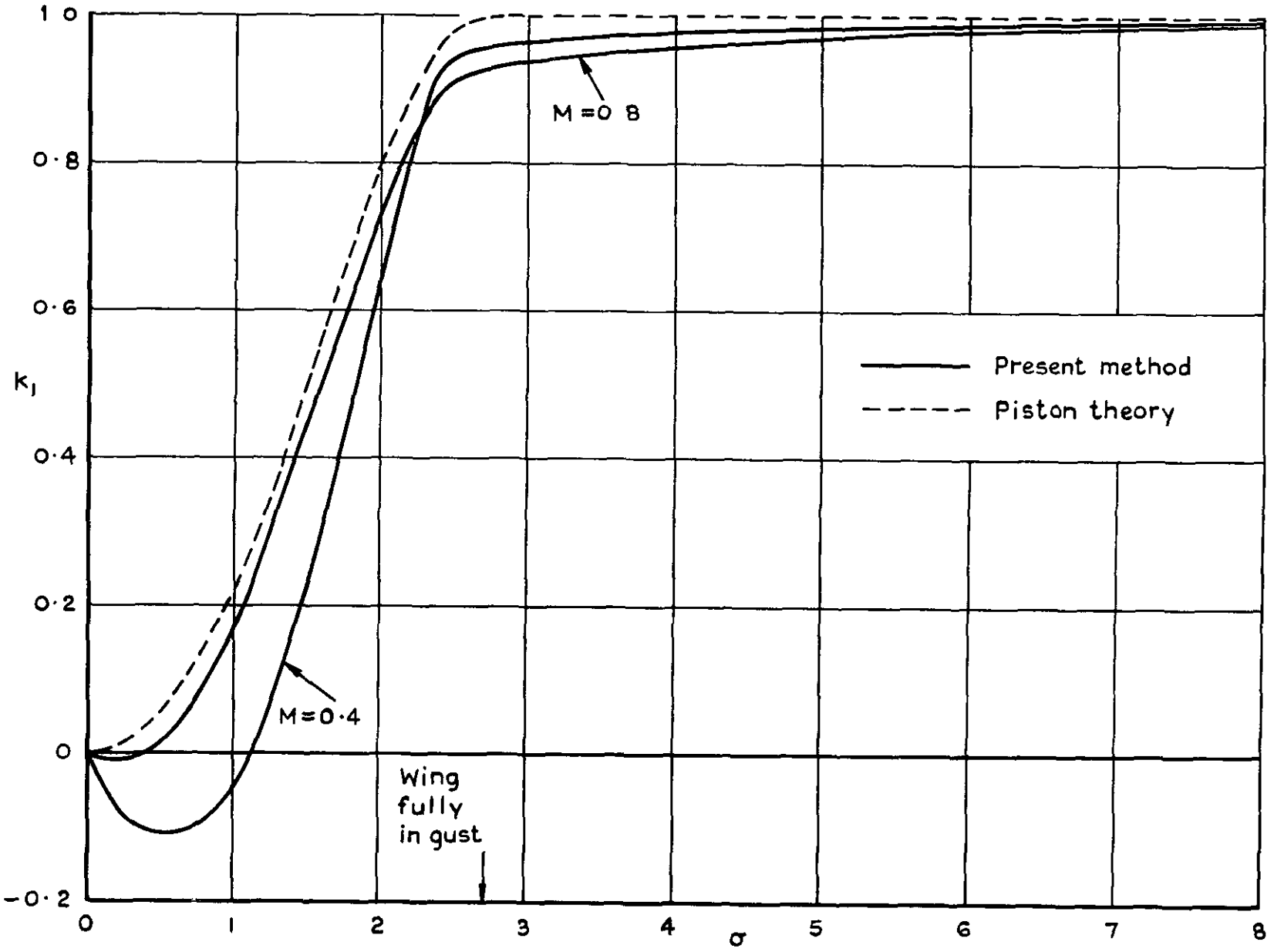

Fig.3 Ratio of transient lift to final lift from a normal step gust

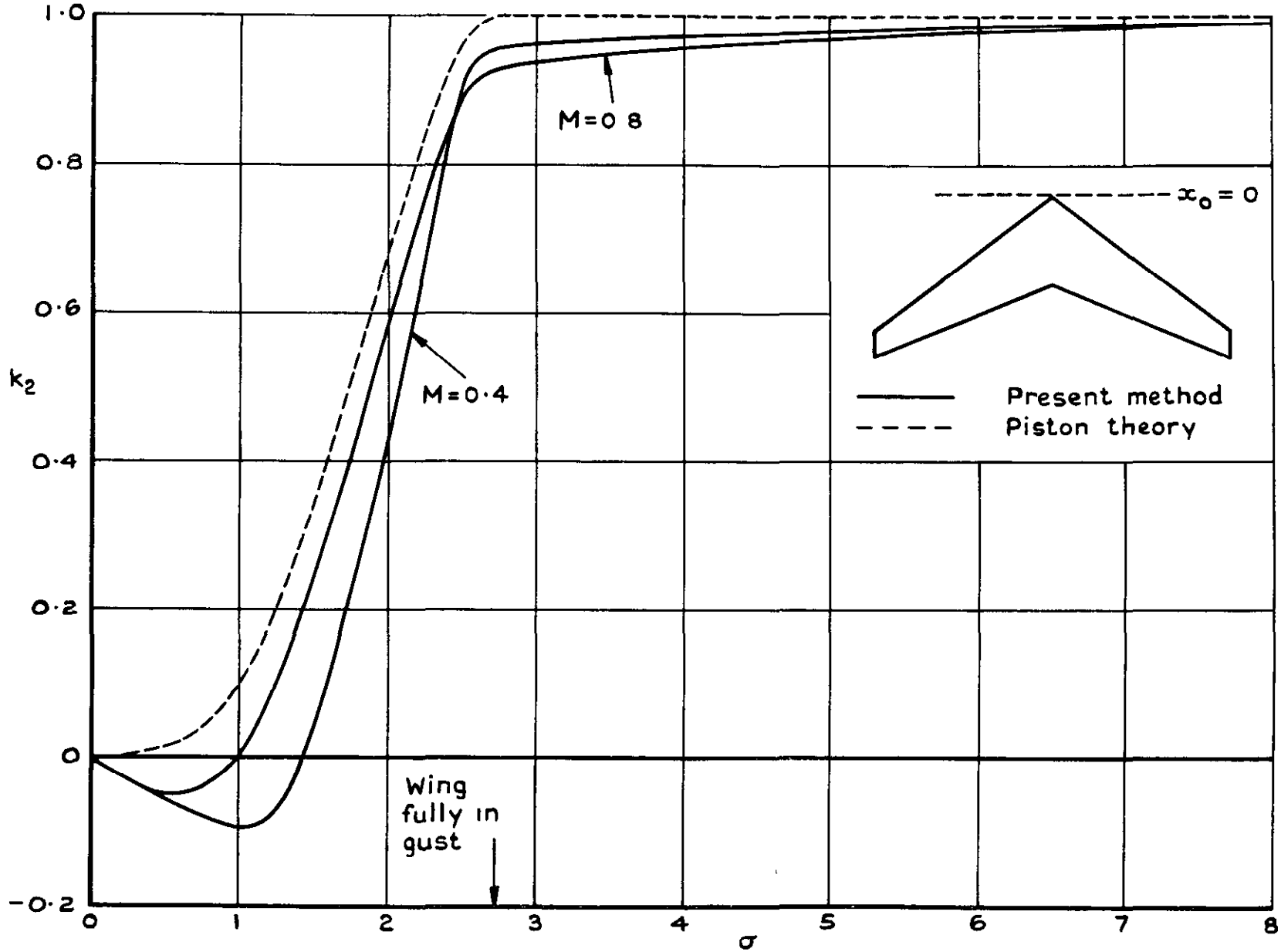

Fig.4 Ratio of transient to final pitching moment from a normal step gust ($x_0 = 0$)

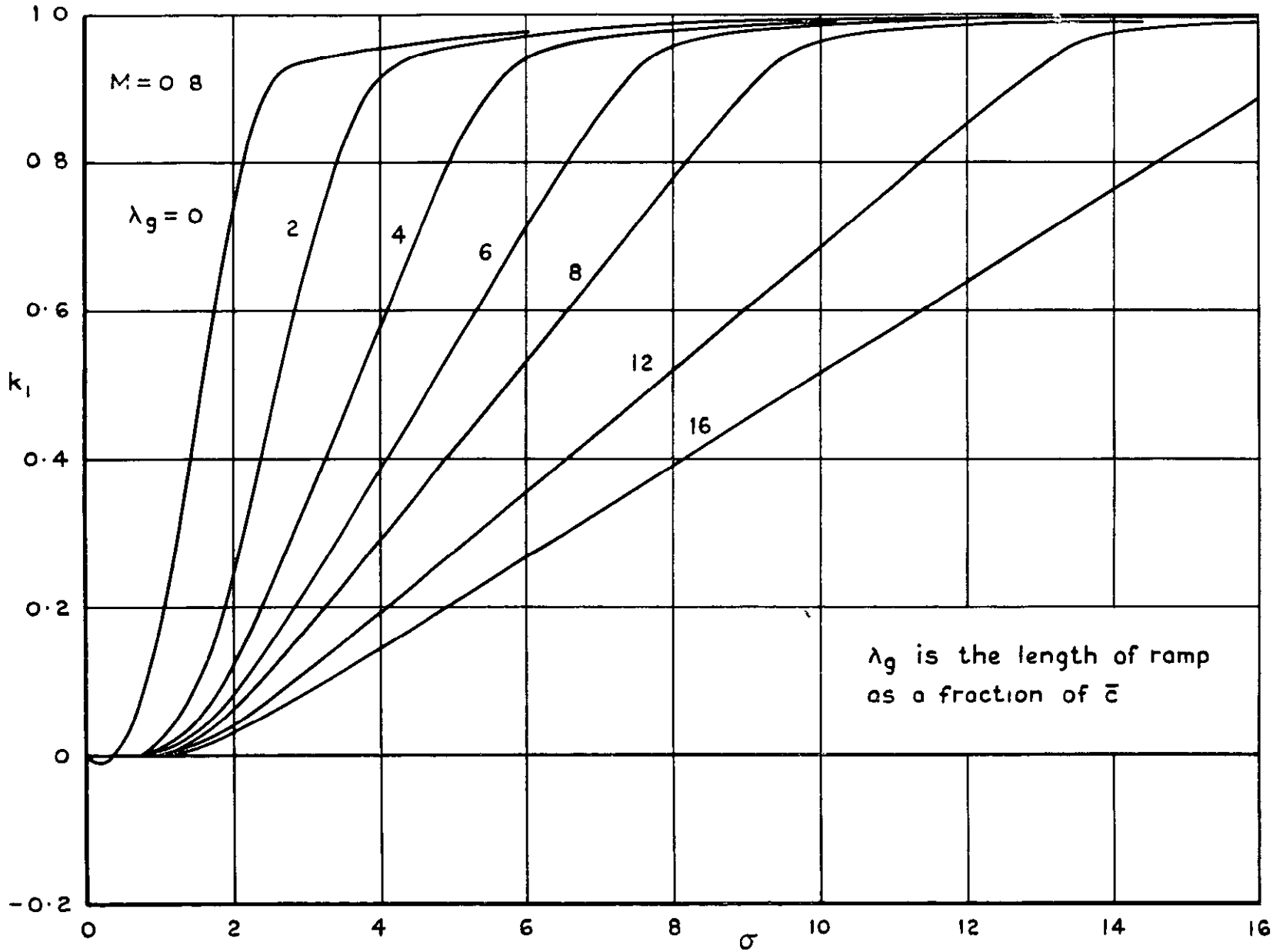

Fig.5 Transient lift ratio from normal ramp gusts (against σ)

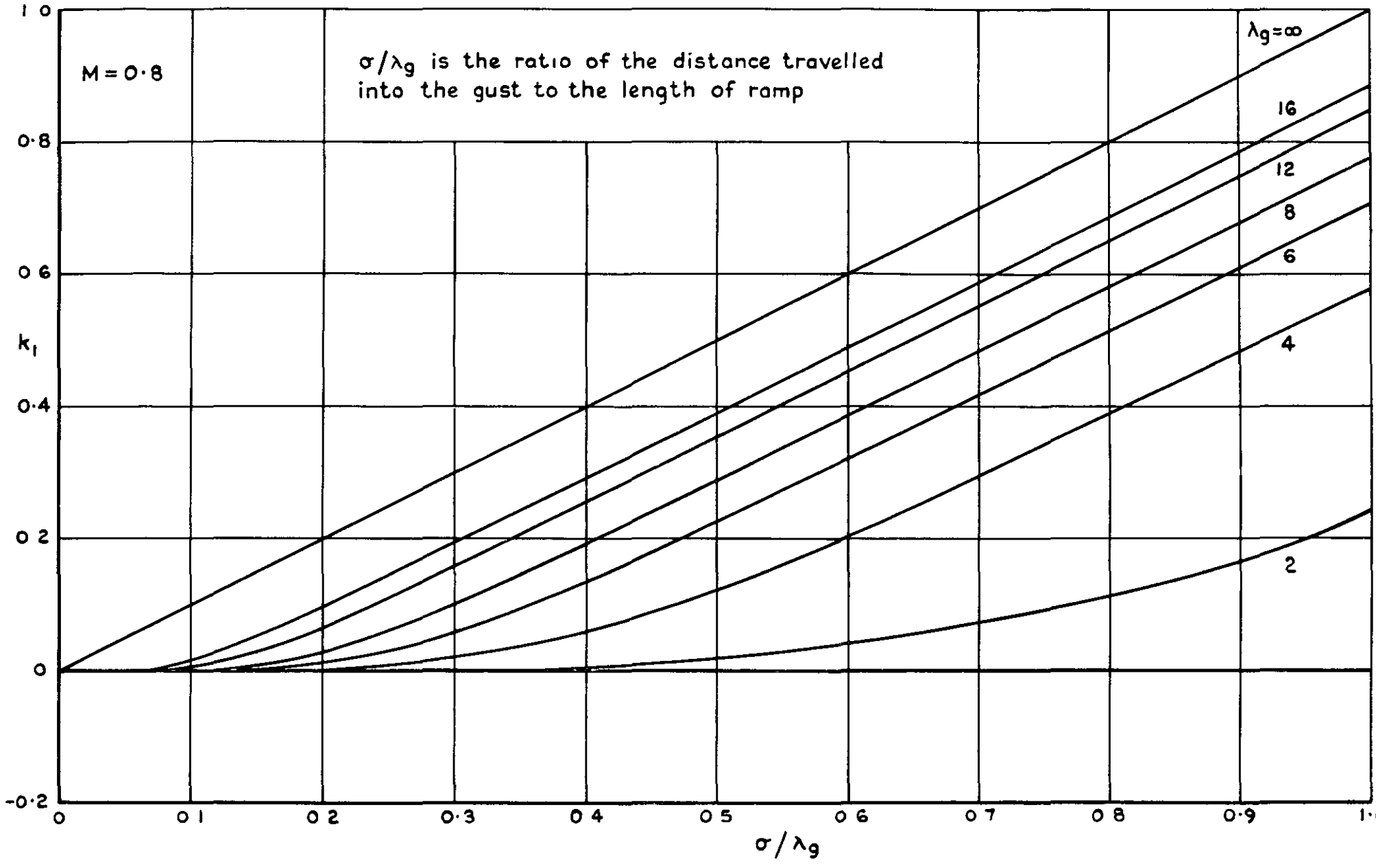

Fig.6 Transient lift ratio from normal ramp gusts (against σ/λ_g)

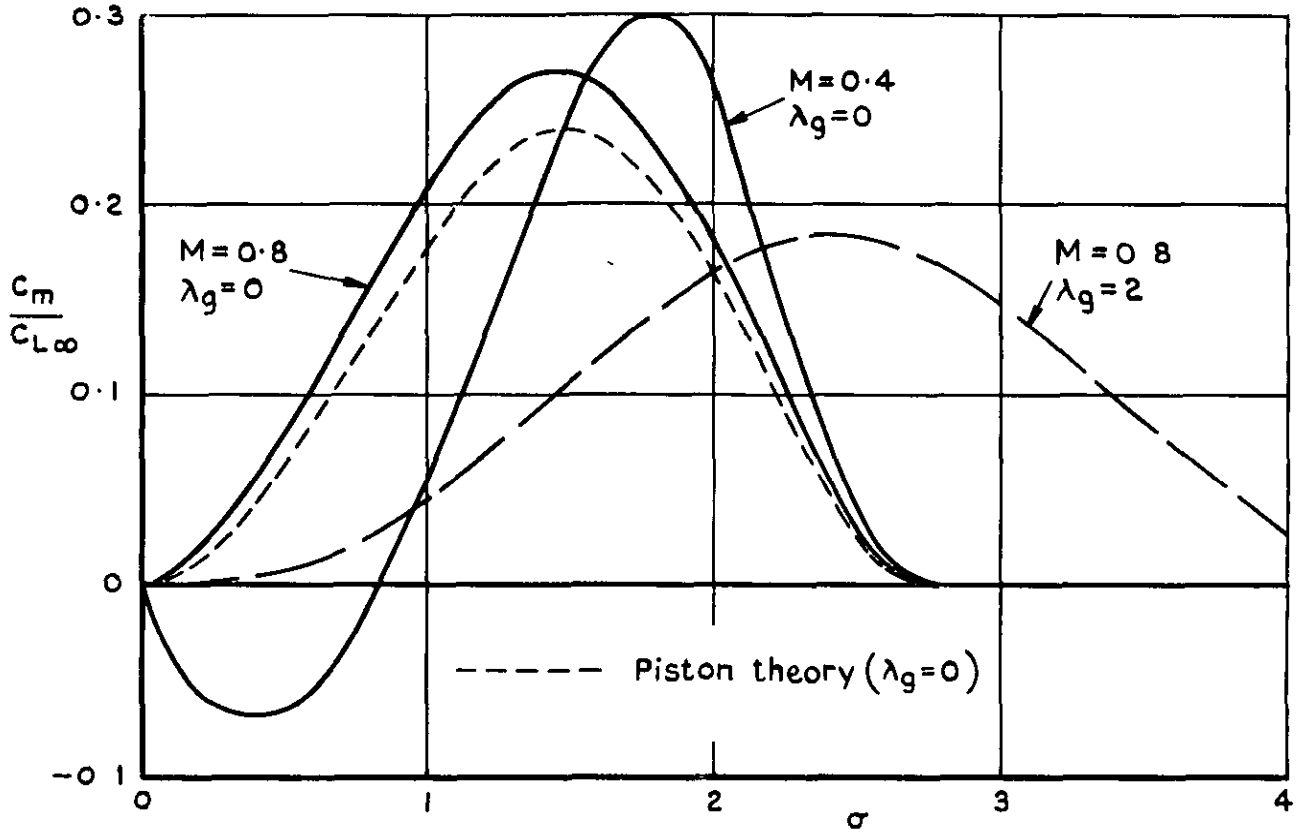

a Effect of Mach number

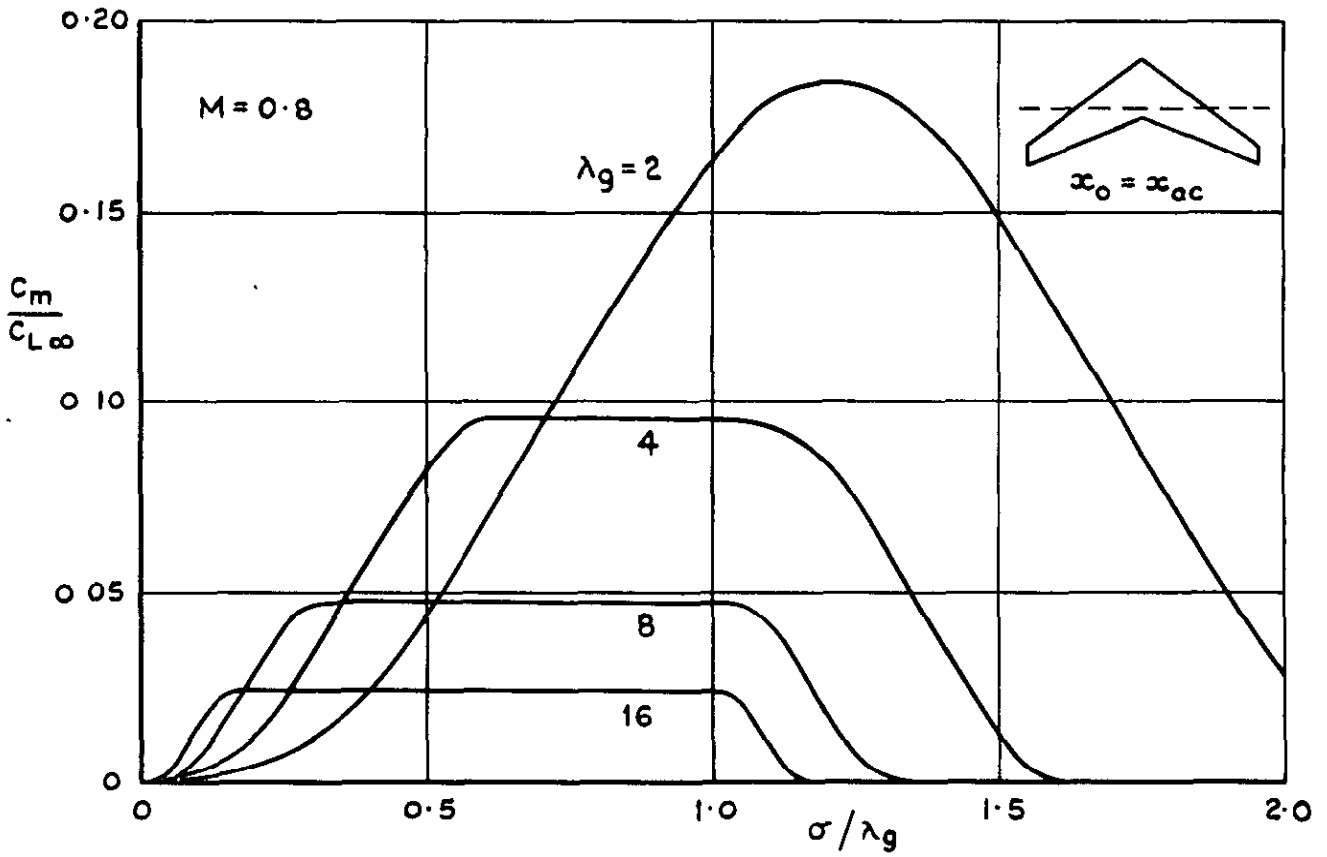

b Effect of ramp length

Fig.7a&b Transient pitching moment about the aerodynamic centre after normal entry into a vertical gust

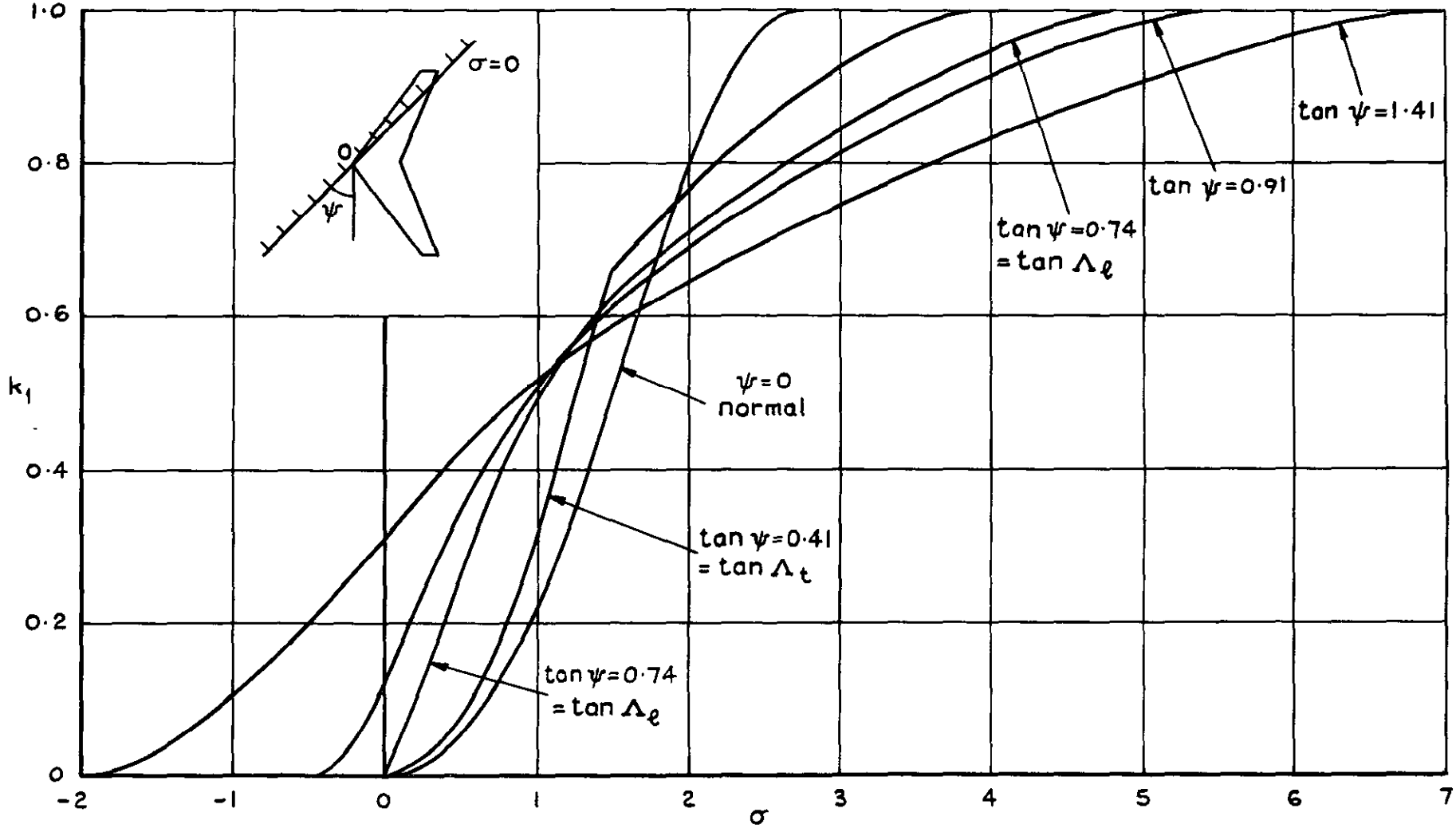

Fig.8 Ratio of transient lift to final lift from oblique step gusts by piston theory

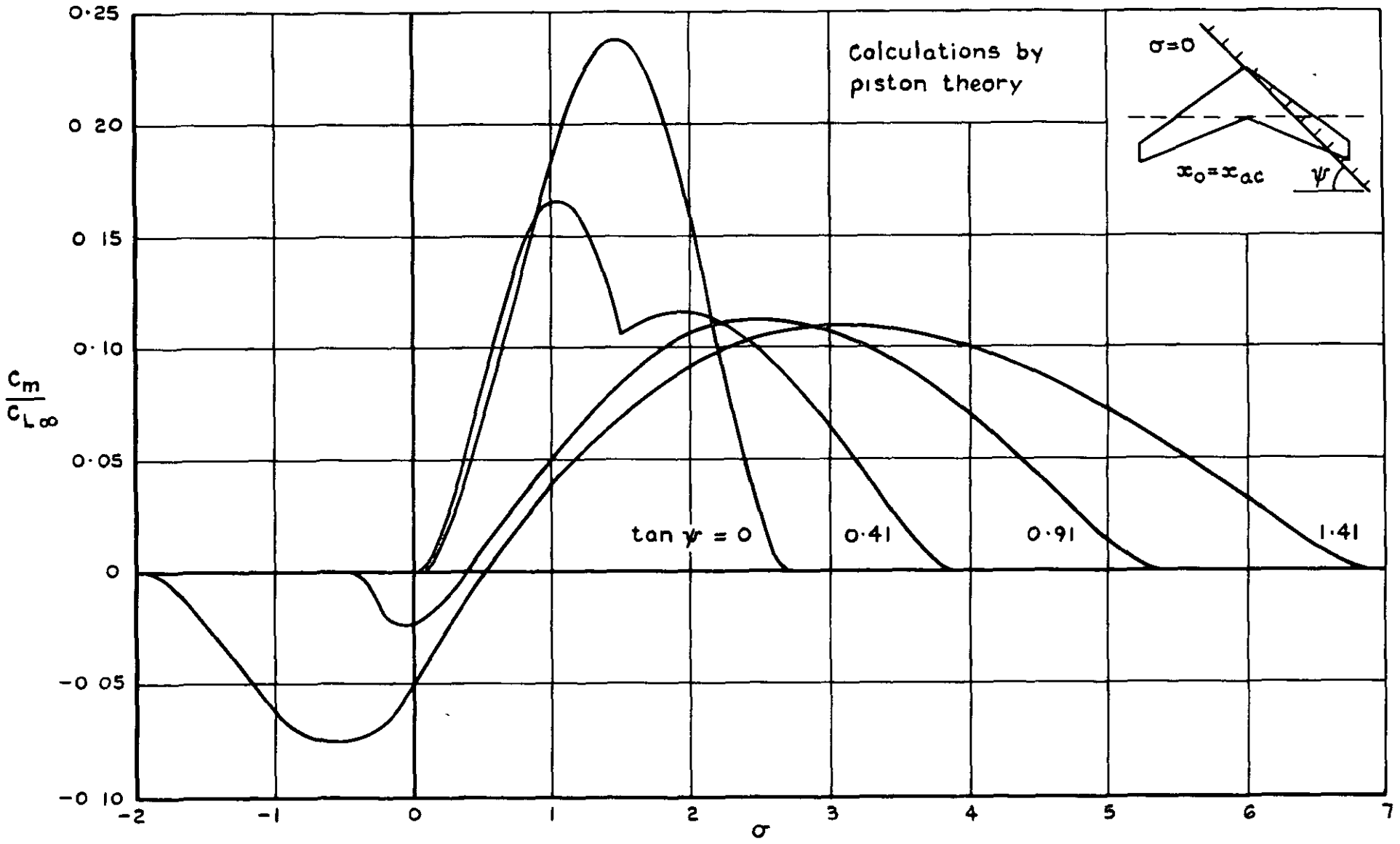

Fig. 9 Transient pitching moment about the aerodynamic centre from oblique step gusts

Printed in England for Her Majesty's Stationery Office by the
Royal Aircraft Establishment, Farnborough Dd 503427 K4 1/73

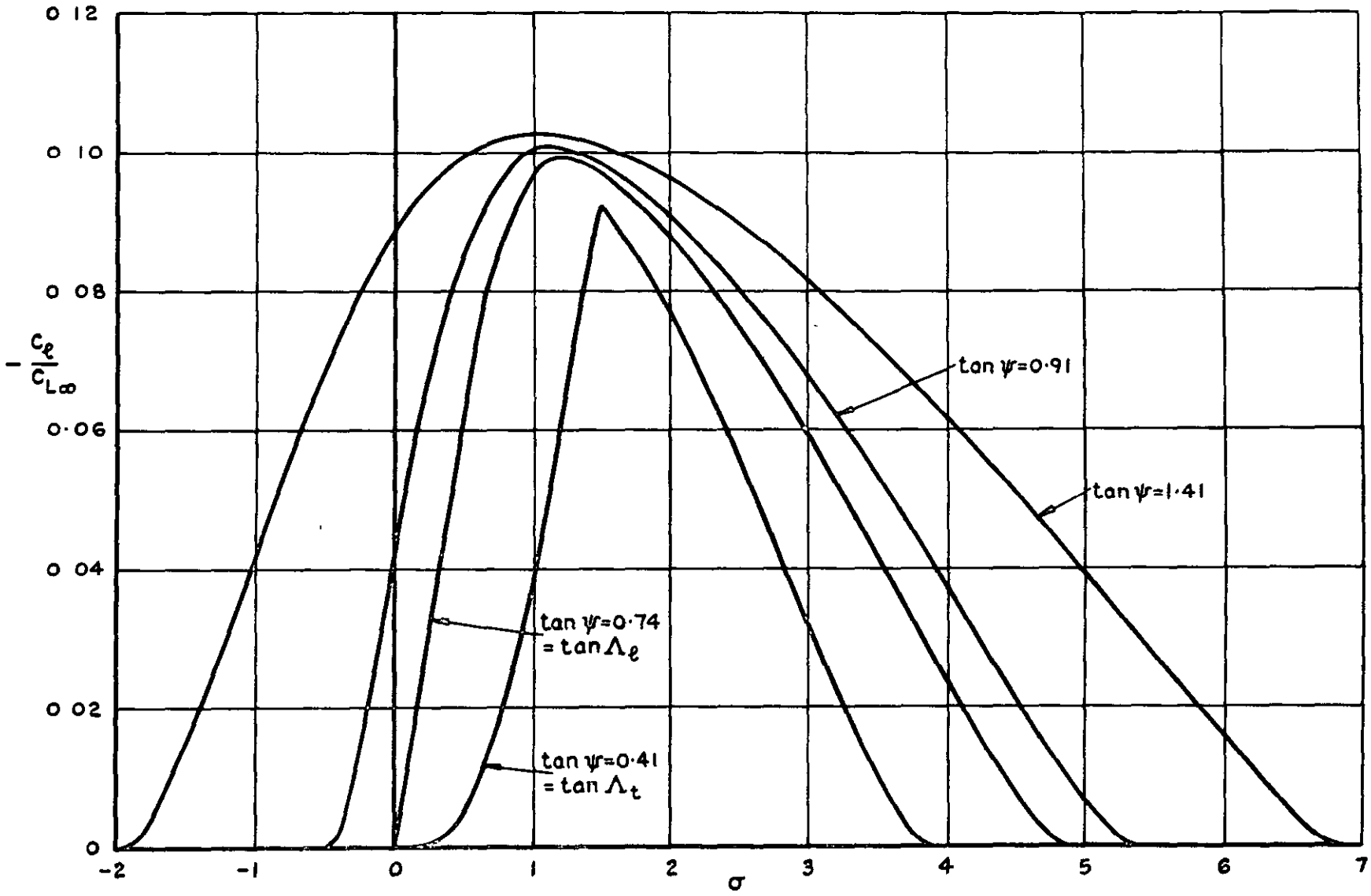

Fig.10 Transient rolling moment from oblique step gusts by piston theory

ARC CP No 1241
January 1972

Garner, H C

533 693 1
551 551
533 6 048 5
533 6 013 13
533 6 013 152

THE CALCULATED GROWTH OF LIFT AND MOMENT ON A SWEPT WING ENTERING A DISCRETE VERTICAL GUST AT SUBSONIC SPEEDS

Unsteady aerodynamic forces on a wing due to a uniform step gust are expressed as a sine transform of those due to sinusoidal gusts over the spectrum of wavelength The sinusoidal gusts are treated by subsonic lifting-surface theory until the wavelength becomes so small as to demand excessive terms in the chordwise loading Beyond this, the substitution of piston theory is discussed for a wing representative of design for subsonic cruise Lift and pitching moment are calculated for normal entry into a step gust at Mach numbers 0 4 and 0 8, with reasonable success in the latter case The results for small distances of penetration are examined critically It is recommended that the proportional growth of aerodynamic force be taken between the results of piston theory and the present method for small distances before approaching the latter result, which leads to the correct asymptotic behaviour soon after the wing is completely immersed in the gust The investigation ends with some calculations by the present method for normal entry into a ramp gust and by piston theory for oblique entry into a step gust

Cut here

ARC CP No 1241
January 1972

Garner, H C

533 693 1
551.551
533 6 048.5
533 6 013 13
533 6 013 152

THE CALCULATED GROWTH OF LIFT AND MOMENT ON A SWEPT WING ENTERING A DISCRETE VERTICAL GUST AT SUBSONIC SPEEDS

Unsteady aerodynamic forces on a wing due to a uniform step gust are expressed as a sine transform of those due to sinusoidal gusts over the spectrum of wavelength The sinusoidal gusts are treated by subsonic lifting-surface theory until the wavelength becomes so small as to demand excessive terms in the chordwise loading Beyond this, the substitution of piston theory is discussed for a wing representative of design for subsonic cruise Lift and pitching moment are calculated for normal entry into a step gust at Mach number 0 4 and 0 8, with reasonable success in the latter case The results for small distances of penetration are examined critically It is recommended that the proportional growth of aerodynamic force be taken between the results of piston theory and the present method for small distances before approaching the latter result, which leads to the correct asymptotic behaviour soon after the wing is completely immersed in the gust The investigation ends with some calculations by the present method for normal entry into a ramp gust and by piston theory for oblique entry into a step gust

Cut here

DETACHABLE ABSTRACT CARDS

DETACHABLE ABSTRACT CARDS

Published by
HER MAJESTY'S STATIONERY OFFICE

To be purchased from
49 High Holborn, London WC1 V 6HB
13a Castle Street, Edinburgh EH2 3AR
109 St Mary Street, Cardiff CF1 1JW
Brazennose Street, Manchester M60 8AS
50 Fairfax Street, Bristol BS1 3DE
258 Broad Street, Birmingham B1 2HE
80 Chichester Street, Belfast BT1 4JY
or through booksellers

C.P. No. 1241

SBN 11 470799 5